

CLASSIFIED DOCUMENT

This document contains classified information affecting the National Defense of the United States within the meaning of the Espionage Act, U.S.C. 1831, and its transmission or the revelation of its contents in any manner to an unauthorized person is prohibited by law. Information so classified may be imparted only to persons in the military and naval forces of the United States, appropriate civilian officers and employees of the Federal Government who have a legitimate interest therein, and to United States citizens of known loyalty and discretion who of necessity must be informed thereof.

CLASSIFICATION CANCELLED

RESTRICTED

TECHNICAL NOTES

NATIONAL ADVISORY COMMITTEE FOR AERONAUTICS

No. 864

THE ELECTRICAL STRUCTURE OF THUNDERSTORMS

By E. J. Workman, R. E. Holzer, and G. T. Pelsor  
University of New Mexico

FOR REFERENCE

NOT TO BE TAKEN FROM THIS ROOM

Washington  
November 1942

# NATIONAL ADVISORY COMMITTEE FOR AERONAUTICS

## TECHNICAL NOTE NO. 864

### THE ELECTRICAL STRUCTURE OF THUNDERSTORMS

By E. J. Workman, R. E. Holzer, and G. T. Pelsor

#### SUMMARY

The time histories of thunderstorm charge distribution during three storms occurring during the summer of 1940 in the vicinity of the Albuquerque airport were investigated by the use of eight synchronized recording electrometers arranged in a particular pattern over a field 1.6 kilometers above sea level. The instruments produced simultaneous records of the changes in the surface potential gradient caused by lightning strokes and each one had a time-resolving power of 0.01 second.

Horizontal and vertical cross-sectional diagrams are presented to show the instantaneous midinterval positions, the signs, and the magnitudes of all charges involved in strokes during specified uniform time intervals. A study of the distribution of the charges showed that it was possible to identify definite regions of charge that persisted for intervals from 10 to greater than 30 minutes. These regions traveled with moving storms and had approximately the same velocity as the heavier rain sheets. In one case where it was possible to compare the average velocity of the charge regions with the average wind velocity at the charge levels in advance of the storm, the two velocities agreed within 10 percent.

#### INTRODUCTION

The study of the distribution of charge in a thunderstorm is of importance both in the problem of determining the fundamental nature of thunderstorm processes and in the consideration of the safety of aircraft. The great complexity of thunderstorms and the difficulties of making reliable experimental observations under thunderstorm conditions have made progress in the field very slow. Since 1929 there have been published the results of a number of investigations (references 1, 2, and 3) that have been carried out in an

attempt to determine the broad features of thunderstorm charge distribution by measurements at the surface of the earth or by measurements obtained from free balloons sent into thunderstorms. These results have been supplemented by observations (reference 4) of pilots who have flown through thunderstorms. In an attempt to obtain a direct quantitative approach to the problem, there has been devised a method of studying charge structure by making simultaneously recorded measurements of the potential gradients and changes in potential gradients at a number of stations at the surface of the earth.

In reference 5 are reported some experiments made in 1939 in which the potential-gradient recorders were of a generating-voltmeter type that had a low time-resolving power. For the experiments described herein, recorders that measure potential-gradient changes with a higher time-resolving power than the first-mentioned recorders were designed and constructed in order to obtain a more complete picture of charge structure. The quantitative results obtained are presented and their bearing on the problems of thunderstorm structure and aircraft safety are discussed. The authors wish to acknowledge the cooperation of the staff at the Albuquerque station of the United States Weather Bureau and, in particular, that of Mr. E. L. Hardy, former official in charge. The writers also wish to express their appreciation of the valuable services of Mr. Herschel Snodgrass for maintenance of the field equipment and aid in the analysis; of Mr. Max Bloakney for assistance in construction of the instruments and in field observations; of Mrs. E. J. Workman for assistance with observations; of Messrs. David Lyon, Lee Jay, John Berger, and Sydney Opie for assistance in laboratory and field.

#### THEORY OF METHOD

Any attempt to determine charge structure above the surface of the earth by means of surface-gradient measurements is based on the assumption that the earth is an extensive conducting body and that the net charge induced on the earth in the vicinity of the cloud is equal in magnitude and opposite in sign to the net cloud charge above the surface. In the simplest case with a single concentrated, or spherically symmetrical, charge above a plane surface of great extent the potential gradient (proportional to the

induced surface density of charge) at any point on the surface of the earth may be calculated simply by the method of electrical images.  $E_i$ , the normal potential gradient at a point on the plane with coordinates  $x_i, y_i$ , is

$$E_i = \frac{2Qz}{[(x - x_i)^2 + (y - y_i)^2 + z^2]^{3/2}} \quad (1)$$

in electrostatic units, where  $x, y, z$  are the space coordinates of the charge and  $Q$  is its magnitude. It is at once evident that, if the charge is to be located above the plane and its magnitude is to be fixed by measurement of surface gradients, the gradient must be simultaneously observed at four points because there are to be determined the four unknowns:  $x, y, z$ , and  $Q$ . The four measurements will yield four simultaneous equations similar to equation (1). In a like manner, if there were  $n$  charges above the plane, all of them could presumably be located and their magnitudes specified by solving  $4n$  simultaneous equations, each having  $n$  terms similar to the right-hand side of equation (1). If  $n$  is a number larger than two or three, even if methods of solution can be devised, the labor involved in the solution of the equations becomes prohibitive.

Fortunately, the thunderstorm itself provides a very important simplifying factor that makes it possible to locate the most significant storm charges. A lightning stroke will, in general, discharge a limited region of charge of one sign in the case of a single cloud-ground stroke and two limited regions of charge of opposite sign in the case of a single stroke within the cloud. If measurements of potential gradients are confined to the charges involved in lightning strokes, the positions and magnitudes of the charges in the regions of greatest activity will be determined and the method of analysis will involve only the location of single charges or charge dipoles. Under these circumstances, charge positions and magnitudes can be determined by gradient measurements at seven stations at the surface. Seven stations can be used instead of eight because the charges of a dipole are equal in magnitude. The calculations involve the solution of seven simultaneous equations. In the present tests eight recording stations were used as a measure of safety to permit analysis in case of failure of one instrument.

Inasmuch as the potential gradient at any point on the earth's surface is the resultant of the gradients produced at that point by all charges in the storm, the part of the gradient due to the charges neutralized by a lightning stroke will be the change in gradient that occurs during the stroke. Many lightning strokes consist of multiple discharges over the same conducting channel at intervals of the order of magnitude of a few hundredths of a second; a gradient recorder capable of resolving one-hundredth second or less is therefore necessary if a large percentage of the strokes of a single storm is to be analyzed. Rapid recorders were therefore designed to resolve the more complicated strokes into single elements draining single charges or dipoles.

#### FUNDAMENTAL ASSUMPTIONS

The location of charge structure by the method described herein involves several assumptions that should be examined.

1. It is assumed that the earth is a conducting plane. The conductivity of the earth has long been established by other methods of measurement and is sufficiently great for the purposes of this study. The following data on topography show that the site chosen for the observations approximated a plane. The instrument field, located to the east of Albuquerque, is about 6 kilometers in diameter and has a maximum difference of elevation of 0.075 kilometer. All the land within 10 kilometers of the center of the field differs from it in elevation by less than 0.25 kilometer. The Sandia range, which reaches an elevation of 1.2 kilometers above the instrument field 15 kilometers to the east and an elevation of 1.7 kilometers above the field 21 kilometers to the northeast, cannot produce appreciable distortion of the measured surface gradients at this distance from the instrument field.

2. It is assumed that the charges are concentrated or spherically symmetrical. It is at once evident that this assumption cannot be exactly satisfied; hence, some estimate of the effect of charge asymmetry should be made. The best evidence for the validity of the assumption lies in the fact that definite solutions are obtained for charge structure involved in a very large percentage of all lightning strokes when this assumption is used. It is of interest,

however, to make some estimates of the volume occupied by a charge.

It may be assumed, for purposes of calculation, that the charge is spherically symmetrical and has uniform density. Under these circumstances the maximum potential gradient, which will occur at the surface of the charge, is given by the relation

$$E = 90 Q/R^2 \quad (2)$$

where  $E$  is in volts per centimeter,  $Q$  in coulombs, and  $R$  in kilometers. If it is assumed, as in reference 6, that the breakdown gradient within the cloud is 10,000 volts per centimeter the maximum radius of any spherical charge of magnitude  $Q$  can be estimated:

$$R = 0.095 \sqrt{Q} \quad (3)$$

A charge of 28 coulombs would have a diameter of about 1 kilometer. The actual volume of the charge would probably be somewhat larger than this value but not of a different order of magnitude.

Several calculations of surface gradients produced by nonuniform distributions of charge within a volume 2 kilometers in diameter and 5 kilometers above the surface were made. The more unfavorable distributions produced surface gradients that differed by less than 10 percent from those due to a uniform charge distribution. The calculations show that at distances of several kilometers above the surface the shape of the charge will not materially affect its location provided that its maximum linear dimension is not greater than 2 kilometers.

3. It is assumed that the only significant charge distributions in the thunderstorm during the short interval of the lightning stroke are the ones that are due to charge transport in the stroke itself. While all the charges in a thunderstorm are space charges in the broadest sense, two types may be distinguished: The charges that are attached to water drops and the charges due to concentrations of atmospheric ions. The mobilities of the two types of charge are enormously different and it may be safely assumed

that during the interval in which a lightning stroke occurs the charges on drops not in the immediate vicinity of the stroke itself are stationary. Laboratory experiments on the mobility of atmospheric ions give values of 1.4 and 1.8 centimeters per second per volt per centimeter for positive and negative ions, respectively. Near the surface of the earth, where the gradients are characteristically of the order of 100 volts per centimeter, the velocities of atmospheric ions would be of the order of magnitude of 100 centimeters per second. During a long stroke, persisting for 0.1 second, the ions would move about 10 centimeters. In general, the ionic displacement will be appreciably less than the displacement just given and will generally produce negligible alteration of the space charge. The velocities of atmospheric ions closer to the charge centers may be 100 or more times greater than they are at the surface, but their greater distance from the recording instruments would make this effect quite negligible.

The possibility remains that a change in gradient at the surface might sweep some of these ions to the electrode of the recording instrument. If it is assumed that the charges in a volume 10 centimeters deep just above the electrode of the field instrument are swept to the electrode during the stroke and if the charge density were great enough to produce a vertical gradient of the potential gradient equal to 1 volt per centimeter per centimeter, the error introduced is 10 percent when the gradient is 100 volts per centimeter. Inasmuch as these assumed values are extreme, this effect can be safely ignored in practice.

#### FIELD APPARATUS

The field apparatus consisted of eight separate recording stations. Each station (fig. 1) consisted of a cylindrical steel tank  $3\frac{1}{2}$  feet in diameter and 6 feet deep provided with a top L that could be lifted and rotated about a vertical shaft S to permit entrance for servicing equipment. The top of the tank was fitted with a circular steel electrode E  $3\frac{1}{2}$  feet in diameter, insulated from the top by means of a wax-covered glass insulator. The recording apparatus R was placed in an offset welded to the tank 2 feet above the bottom. The recording apparatus consisted of a quartz-fiber string electrometer, electrometer batteries, a 500-watt projection lamp, a condenser lens for illuminating the fiber, a recording camera, and a synchronous motor and gear train

for driving the film. The electrometer fiber was connected to the electrode above the tank by a metal chain and also to ground through a 1000 megohm resistance, so that it remained at ground potential except during rapid changes in the potential gradient at the electrode. The time constant of the electrometer system was thus adjusted to approximately 1 second and the period of the electrometer to approximately 0.01 second. The deflection of the electrometer was magnified 10 times by the achromatic lens of the recording camera.

The camera magazine held 100 feet of 16-millimeter motion-picture film that was driven continuously at the rate of one frame (0.3 in.) in 2.4 seconds; when the film image was magnified 20 times, intervals of one-hundredth second could be observed without difficulty.

Each tank was buried in the ground in such a manner that the electrode was approximately at the level of the surrounding terrain. The recording apparatus in the offset 4 feet below the surface was not subject to large diurnal temperature fluctuations and no difficulty with changing electrometer calibration or battery voltages was experienced.

The power supply for each tank station was 115-volt alternating-current. Within the tank the alternating-current leads, the plugs, the lamp, and the motor were carefully shielded from the electrometer system. Outside the tank, the leads were buried a few inches in the ground and carried to a switch at a power line not less than 400 feet from the tank, so that the power line was never higher than  $5^\circ$  above the horizon when viewed from the tank. A space 40 feet in diameter around each tank was cleared of wild grass and other small plants to eliminate local irregularities.

The calibration of the instrument to read changes in potential gradients was accomplished in the following way. First, a voltage calibration of the electrometer was obtained. Then a circular screen 14 feet in diameter was mounted parallel to the top of the instrument. A definite potential difference was established between the screen and the electrode; and the electrometer deflection was observed when the screen potential was suddenly reduced to zero. Repeated tests were made with a wide range of potential differences and screen-electrode separations. The ratio of potential-gradient changes at the electrode to potential changes of the electrometer (a constant) was thus determined.



Thereafter, it was necessary only to check the voltage calibration of the electrometer. During the period when observations were made, the voltage calibration and a check of the time constant of the electrometer system were made within a few hours of each storm for which measurements were obtained.

### FIELD PROCEDURE

On days when thunderstorms were expected, an observer was stationed at the tower of the administration building at Albuquerque municipal airport. When a thunderstorm development within an hour seemed probable, the observer called the field crew of three to their respective stations. When a thunderstorm that might influence the field instruments was imminent, the observer ordered the instruments turned on. The time required to start the eight instruments was usually from 8 to 10 minutes. At the close of the storm, the field crew was directed to turn the instruments off. The field crew recorded the time to the nearest second when each instrument was turned on and off to facilitate subsequent synchronization of records.

The observer and an assistant meanwhile recorded pertinent storm data, such as position of cloud; development of rain sheets; position, time, and character of lightning; time and duration of thunder; storm motion and miscellaneous observations. The recording was greatly facilitated by a specially constructed recorder carrying a 6-inch paper tape driven by a synchronous motor. With this recorder a single pencil stroke in the appropriate column on the tape was sufficient to record the time of any event and the assistant was left free to make special notes.

### METHODS OF ANALYSIS

All the data for determining potential-gradient changes at each instrument were obtained from the photographic films giving a continuous record of the deflection of the electrometer fiber. For the purpose of reading the film records and determining the time, a Kodascope Model D projector was fitted with a gear train to turn indicator disks in order that the

time of any event projected on the screen could be read directly. The projector was provided with a Taylor-Hobson Cooke lens with a focal length of 1 inch and an aperture of  $f/1.5$ . The image of the recorder trace was magnified 20 times for ease in reading. The flatness of the field was checked. The calibration data indicated that the fiber displacement was approximately proportional to its potential and, to the same extent, proportional to changes in potential gradient.

When no rapid change in the potential gradient occurs, the electrometer trace is a straight line. When the gradient change occurs in less than 0.01 second, the trace resembles that of figure 2 (a), where AB measures the sudden change in electrometer potential and BC is an exponential-decay curve determined by the time constant of the system. In this case AB is proportional to the change in potential gradient to a high degree of approximation.

When the gradient change is slow, occupying several hundredths to several tenths of a second, the trace resembles figure 2 (b). The maximum electrometer deflection EF is no longer proportional to the gradient change in the interval DF, since charge was leaking off during the interval. Corrections for this leakage may be made in the following manner: If no leakage had occurred, the deflection (potential change at the electrometer) would have been greater than that ob-

served by the amount  $\frac{1}{RC} \int_D^F V dt$  where R is the re-

sistance to ground, C the capacitance of the electrometer system, V the electrometer potential, and t the time. The

gradient change is then proportional to  $EF + \frac{1}{RC} \int_D^F V dt$

and the correction term is proportional to the area DEF. Graphical methods employing the calibration data were devised to make corrections when necessary. Figure 3 shows contact prints of the original film records for characteristic gradient changes occurring during lightning strokes.

When the data for a single storm were analyzed, the records of the separate instruments were synchronized with each other and with the observer's record. Corresponding

gradient changes were then determined for each of the eight instruments and for every possible stroke element.

The next step was to determine the charge structure neutralized by a lightning stroke that produced the observed gradient changes. If the individual gradient changes were known with mathematical accuracy, it might have been possible to develop a mathematical procedure for solving eight simultaneous equations without too much labor. Since the magnitudes of the gradient changes in different parts of the field differed by factors of 2 to 20, however, the percentage accuracy with which the gradient changes could be measured varied widely, amounting to 20 percent or more for some of the smallest changes. It was, therefore, impossible to obtain a unique solution for a set of data: there was obtained instead solutions that grouped themselves around a most probable value. Preliminary work on a few solutions was done by a series of successive approximations. In each attempt to obtain a solution a charge structure was assumed, the gradients produced by the charge structure were calculated, and the calculated gradients were compared with the observed gradients. The process consumed a large amount of time and depended greatly on the skill of the analyst. It was therefore decided to build a mechanical analyzer that would enormously speed up the process of approximating a solution.

#### DESCRIPTION AND USE OF THE ANALYZER

The analyzer, constructed for the purpose of determining the charge structure that produced any given set of gradients at the recording instruments, is shown in figure 4. Essentially, the instrument consisted of two sets of eight pins that could be displaced vertically. Each set had the same relative horizontal position, on reduced scale, as the field recorders. Curved metal surfaces, which represented the horizontal distributions of the potential gradient under a charge of definite height, could be moved about under each set of pins. The differential displacement of pin pairs (one from each set, corresponding to one field recorder) was transmitted to a group of eight dial gages by a system of levers. The gage readings indicated when a solution had been obtained. The location of the charge structure could be determined from the positions of the curved surfaces and the particular pair of surfaces used. The details of its construction, operation, and use are given in the following paragraphs.

The instrument bed was a steel channel iron with a surface 12 by 30 inches planed to within less than 0.001 inch. A steel plate 18 inches square was mounted perpendicular to the instrument bed on a substantial cast-iron bracket. The lower edge of the plate was parallel to the bed and 4.5 inches above it. There were eight sets of moving parts, similar in design, one set of which is shown in figure 5. The surfaces  $S$  and  $S'$  were made of cast-aluminum piston alloy and were turned on a lathe to an accuracy of 0.001 inch. Allowance for the shape of the pins ( $P$ ,  $P'$ ) was made in turning by making the lathe-tool profile the same as an axial section of the pin. The surfaces were 7 inches in diameter. Their horizontal scale was 4 kilometers to the inch and their vertical scale was 2000 volts per centimeter to the inch. Each was constructed for a 100-coulomb charge at a definite height above the surface of the earth, and the shape of the surface represented the horizontal distribution of the gradients under the charge. In use, the surfaces were free to move over the steel bed  $B$  at any position under the sets of pins. Coordinate systems were scratched in the steel bed under each set of pins so that the horizontal displacement of the center of the surface from the center of the instrument field, that is, the middle pin, could be read directly.

Since the surfaces  $S$  and  $S'$  each represents a charge of one definite height, it was necessary to have several surfaces for charges at various heights. Eighteen such surfaces - nine convex and nine concave - were constructed for heights from 3 to 7 kilometers at half-kilometer intervals. Previous tests had shown this range to be the one in which most lightning stroke charges were found. Figure 6 is a photograph of three convex surfaces for 100-coulomb charges at 3, 4, and 5 kilometers. The marked change in the shape of the surface with charge elevation in this range of charge heights is well illustrated.

Now, when a surface  $S$  corresponding to a 100-coulomb positive charge at height  $z$  was located so that its horizontal coordinates with respect to the center of the field were  $x$  and  $y$ , and when a surface  $S'$  corresponding to a 100-coulomb negative charge at height  $z'$  was located so that its horizontal coordinates with respect to the center of the field were  $x'$  and  $y'$ , the algebraic sum of the displacements of  $P$  and  $P'$  (each corresponding to the same field instrument) measured the resultant gradient at this instrument due to the charge dipole: +100 coulombs at  $x$ ,  $y$ ,  $z$  and -100 coulombs at  $x'$ ,  $y'$ , and  $z'$ . This resultant gradient was

proportional to the displacement of the midpoint  $M$  of a connecting bar  $C$  mounted on knife edges in slots through the pins  $P$  and  $P'$ .

The midpoint  $M$  was connected by a link  $L$  to the end point  $N$  of a ratio arm  $R$  which had a horizontal axis at  $O$ . The arm  $R$  turned on a shaft supported by a bearing in the vertical plate  $V$ . Above the ratio arm a fixed bar  $F$ , also supported by the plate  $V$ , carried an Ames dial gage  $D$  in a special mount so that it could be moved to any point  $K$  on the ratio arm. The dial reading was now  $E' = \left(\frac{KO}{NO}\right)\left(\frac{E}{2}\right)$  where  $E$  was the algebraic sum of the displacements of the pins  $P$  and  $P'$ .  $E$  is the resultant gradient for the 100-coulomb dipole, represented by the surfaces  $S$  and  $S'$ , at the recorder represented by the pins  $P$  and  $P'$ .

The other seven assemblies representing the other seven field recorders were similarly constructed. For any given dipole position, the condition that all the gages have the same deflection was that  $KO \propto 1/E$ . Conversely, when each of the various arms similar to  $KO$  was made inversely proportional to observed gradient changes at their respective instruments, the position of the structure responsible for those gradient changes was indicated by the surfaces used and their positions when all the gages had the same deflection. Since  $E$  is the gradient for a 100-coulomb dipole,  $E_Q$  the gradient for a  $Q$ -coulomb dipole in the same position would be  $E_Q = Q/100 E$ . It follows that charge of the dipole under consideration is  $Q = \left(\frac{KO}{NO}\right)\left(\frac{EQ}{E'}\right)$

The procedure ordinarily used in determining a charge structure was as follows:

1. A group of corresponding gradient changes for the eight instruments was selected. The reciprocals of the gradient changes were calculated and the  $K$  positions were set so that the distances  $KO$  were proportional to the reciprocal gradients.
2. Two flat plates were placed under the pins and the gage zeros were checked.
3. The operator examined the gradient pattern and decided, on the basis of the symmetry of the field and the

relative gradient magnitudes, whether the charge structure was apt to be a dipole or a single charge. He also estimated the probable charge heights. A skilled operator could make a good approximation on the first attempt.

4. One flat surface and one curved surface were used for a single charge and one concave and one convex surface were used for a dipole.

5. The operator adjusted the horizontal position of the surfaces while observing the dial gages. If the selected surfaces failed to give a solution, the gage readings usually suggested the surfaces that should be tried next. Successive trials were made until a range of approximate solutions was obtained.

#### ACCURACY OF ANALYSIS

It is difficult to assign a simple probable error to the results of the analysis. A more satisfactory method of indicating the accuracy of the results is to describe the tolerances allowed in obtaining a solution and the spread of the results that were accepted as solutions.

It was possible to determine gradient changes on each instrument within less than 0.5 volt per centimeter. The percentage accuracy of each reading in a set then depended upon its absolute magnitude. The operator was guided in seeking a solution by the fact that the allowable deviation of any particular gage reading from the others when a solution was approximated was directly proportional to the ratio-arm setting. When a group of solutions for a set of data had been obtained, the most accurate (as determined by the equality of the gage readings) was selected. The mean deviation of the various solutions in a given set from the accepted solution was approximately 1 kilometer in horizontal charge position and 0.5 kilometer in vertical position. Among a group of acceptable solutions, the charge magnitude varied with the position coordinates of the charge. For single charges (neutralized by cloud-ground strokes), or for dipoles with large separation (neutralized by intracloud strokes), the charge magnitudes varied about 20 percent with charge positions for the various acceptable solutions. In the case of short dipoles, the charge magnitude associated with a solution was very sensitive to charge separation, which is to be expected because the dipole moment is the product of the

charge and the charge separation. Dipoles with small separation (1 km) are relatively infrequent, however, and the charge averages are not materially affected by this uncertainty.

### RESULTS OF STROKE ANALYSIS

Three storms occurring on August 15, September 3, and September 10, 1940, respectively, were analyzed. Analyses were attempted for 312 stroke elements and 187 satisfactory solutions were obtained. Tables I, II, and III give the time, the type of stroke, the position coordinates of the charges, and the charge magnitude for the successful analyses. The letters following the time of the stroke designate the particular stroke element. The charge coordinates are all measured in kilometers distance from the center of the instrument field. The positive x-axis is east, and the positive y-axis, north. The coordinate z is the distance above the surface and its sign represents the sign of the charge to which the set of coordinates applies. It should be noted that the surface of the instrument field is 1.6 kilometers above sea level. The charge magnitudes are given in coulombs.

Satisfactory solutions were obtained for 60 percent of all sets of data attempted. The causes of failure to obtain satisfactory solutions in the other 40 percent of the cases are summarized as follows:

1. In 22 percent of the cases, the gradient changes at several, or all, of the instruments were so small that the error in reading the electrometer deflection precluded a unique solution.
2. In 3 percent of the cases, electrometer deflections of two or more instruments were off scale and could not be extrapolated.
3. In 7 percent of the cases the record on two or more instruments was illegible or otherwise indeterminate.
4. In 8 percent of the cases, the data obtained were apparently adequate but failed to fit any simple charge distribution. In the latter cases it appears that the assumption of a single concentrated charge or two concentrated dipole charges is not satisfied. The most likely

causes of the failure of this assumption are the development of a large branch of the lightning stroke that would carry charge over an irregular and extensive volume and the development of an air discharge, that is, a lightning stroke which extends into the region below the cloud base but does not reach the ground.

The time between the lightning flash and the thunder was observed in the case of a large number of strokes analyzed and offers an independent check on the accuracy of the location of charge positions. There are a number of situations in which thunder observations are equivocal. If two strokes occur a few seconds apart, the thunder from the two may overlap. If a nearby stroke occurs after a more distant stroke, it is frequently impossible to determine the thunder time for the distant stroke, or for either stroke, in case both strokes are at considerable distances from the observer. After all doubtful records have been discarded, there is still a large percentage of cases in which thunder can be clearly associated with a particular stroke. The distance in kilometers from the observer to the nearest portion of the lightning channel was obtained by dividing the thunder interval, in seconds, by 3. This distance was compared with the distance from the observer to the nearest portion of the charge structure or, in some cases, the nearest portion of the straight line joining the charges of a dipole. That this comparison cannot be exact is at once clear, since lightning strokes do not travel in straight lines and since some strokes have branches of considerable length. The two calculations agreed, however, within 1 kilometer in 47 percent of the cases, within 2 kilometers in 62 percent of the cases, and within 3 kilometers in 80 percent of the cases. The remaining 20 percent of the cases with 3- to 5-kilometer deviations were all distant strokes and the observer may have failed to distinguish the first thunder.

The observer also recorded the range of azimuth angles subtended by the observed lightning stroke or the region of cloud-base illumination in the case of intracloud strokes. Because of the irregular nature of the lightning channel, and particularly because of the unknown course of the channel when obscured by clouds, precise agreement cannot be expected.

It is, however, interesting to note that the direction of the calculated charge structure and the observed stroke or cloud illumination were generally less than  $10^\circ$  apart.



Since the thunder and angle checks are quite independent of the electrical measurements and analysis, they constitute a verification of the essential correctness of the analysis and the validity of the fundamental assumptions underlying the analysis.

Average values for charge data, computed for the strokes analyzed, are of interest in that they give a reliable order of magnitude. The average charge neutralized by a stroke element is 6.5 coulombs and the average value of the charge neutralized by a lightning stroke (the sum of the separate charges neutralized by the various elements of the stroke in the case of repeated strokes) is 24 coulombs. The effect of the small unanalyzed elements has been estimated and compensated for in computing the averages.

Average values of charge heights and horizontal-charge spacing are not affected as much by the elimination of the group of small charges as are charge-magnitude averages, since there is no a priori reason to assume that the unanalyzed charges are at a characteristically different height from those charges analyzed. Further, a comparison of the original data for the strokes analyzed and those not analyzed shows that the ratios of maximum to minimum gradient changes observed for each stroke are not sensibly different, which indicates that the charges lie in the same range of heights above the surface. The striking effect of the height of the charge on the surface-gradient distribution is well shown by the contours of the plates in figure 6.

The weighted mean height of the negative charges above the surface was 5.2 kilometers and of the positive charges is 5.8 kilometers. The weighted mean horizontal separation of charges involved in an intracloud stroke was 3 kilometers. The heights of both positive and negative charges ranged between 4 and 7 kilometers while the horizontal separations varied from 1 to 10 kilometers.

In the three storms studied, cloud-ground strokes were observed only on August 15. All these strokes transported negative charge to ground. The writers had made this same observation for several storms in 1939. Also, tests were conducted in 1941 with a single sensitive generating voltmeter. If a cloud-ground stroke only transports negative charge to the ground, the gradient change at all observing

stations on the ground, however distant, must be positive. Approximately 100 cloud-ground strokes in the 1941 season all produced positive gradient changes, regardless of the distance of the stroke from the observing station. Intra-cloud strokes produced gradient changes of both signs, depending on their position with respect to the observing station.

It is interesting to note that in the case of a stroke that an observer would classify as a cloud-ground stroke, some elements may transport negative charge to ground, but one or more elements not visible to the observer may discharge dipoles within the cloud. In the storm of August 15, for example (table I), the strokes occurring at 6:35:13 and 6:48:20 are of this type. Even though more negative than positive charge is neutralized in a stroke of this type, there is in some cases a small region at the surface where negative rather than positive gradient changes would be observed. This result clearly indicates that conclusive evidence of transport of positive charge to ground in a cloud-ground stroke could not be obtained with a single recorder. It is possible that there are some circumstances in which cloud-ground strokes carry positive charge to ground. If such strokes do exist, however, they are rare.

#### CORRELATIONS WITH METEOROLOGICAL DATA

After a charge analysis had been checked against thunder and position observations on the individual lightning strokes and after the purely statistical study of the results had been made, an attempt to correlate the results with meteorological conditions in the storm was made. This attempt led to a number of interesting results.

If the charge analyses of the separate storm strokes are to be used for locating regions of charge within clouds, several considerations must be borne in mind. If the charge region in a cloud is extensive, a single stroke with its separate elements may discharge only a part of the region. If an attempt at a more careful delineation of the region is made by plotting the positions of several successive strokes that occur in a definite interval of time, the storm motion during the interval may produce apparent distortion. Further, if two charge regions are adjacent, the storm motion during the interval may create apparent anomalies by making the region boundaries indeterminate. In order to eliminate

these difficulties and determine the approximate boundaries of charge regions, the following procedure was adopted. All the charges in a given storm were plotted on a chart with the value of either the  $x$  or the  $y$  coordinate plotted against time. The remaining horizontal coordinate ( $y$  or  $x$ ) was then indicated by a number entered on the chart beside the charge. Figure 7 illustrates the method as used to study the negative charges of the storm of August 15. The  $y$  coordinates of the charges are plotted horizontally and the time is plotted vertically. The numbers entered on the chart represent the  $x$  coordinates of the charges. Examination of the diagram shows that there are three groups of charges with similar  $x$  coordinates in any time interval that lie in bands sloping downward and to the right. Each band represents one region of charge moving with the storm. The slope of the band, indicated by the sloping dashed lines, is a measure of the  $y$  component of the velocity of the region. The  $x$  components of the velocities of the regions were determined in a similar manner. The same procedure was used for both positive and negative charges in each storm and the negative regions in each storm were designated by odd numbers, the positive regions by even numbers.

Horizontal diagrams were then plotted for a definite time in the middle of the interval to be represented. Each charge occurring within the interval was displaced so that its plotted position was the position it would have had at the instant for which the diagram was plotted rather than the position of the charge at the time the lightning stroke occurred. It was assumed that the velocity of the region as determined by the method just described and essentially constant for all parts of the region. Both horizontal and vertical diagrams of the charge positions were prepared in this way for the three storms studied. These diagrams are shown in figures 8, 9, 11, 12, and 14. In addition, two diagrams, figures 10 and 13, showing the mean horizontal paths of the charge regions have been prepared.

In all the horizontal diagrams, the positive and the negative charges neutralized by the same intracloud stroke were connected by straight lines except in the case of the storm of September 10. In all the vertical diagrams, negative charges neutralized by cloud-ground strokes are connected to ground by a vertical line. All the diagrams exhibiting horizontal distribution of charges show the origin of the coordinate system (the center of the instrument field) 0 and the airport tower AP, where the observer was stationed. All the vertical diagrams show, in addition to the origin

of coordinates, the cloud base CB and the vertical distribution of temperatures calculated as described in the following paragraph. On each diagram, horizontal or vertical, the length of the interval is that during which the plotted charges were neutralized by strokes.

The meteorological data for the storms consisted partly of visual observations and partly of data supplied by the Albuquerque station of the United States Weather Bureau. Table IV gives the elevation of the condensation levels and the various isothermal surfaces in the three storms. The vertical distribution of temperature was calculated by use of the surface temperature and the humidity immediately before the storm and by assumption of a dry adiabatic lapse rate until the condensation level was reached, and a psuedoadiabatic lapse rate within the cloud. The condensation level agrees well with observed elevation of the cloud base at the beginning of the storm.

Table V gives the mean charge heights above the surface for each storm day and the temperature range in the region where charges were found. Table VI shows the vertical distribution of the winds at 3:00 p.m. on each storm day. The observations on September 3 were made as the storm approached the Weather Bureau station and ceased at the point where the pilot balloon entered a cloud (not the base of the storm). These observations are, therefore, less complete and reliable than the observations for the other 2 days.

The azimuth angle subtended by the rain sheets at the airport station are recorded on the diagrams showing horizontal charge distribution. Within the angle, the time of the observation and the character of the rain sheet are indicated. On the charts, L indicates a light or translucent rain sheet and H indicates a heavy or opaque rain sheet.

The results of the analysis of the charge distributions and meteorological data are summarized by storms.

#### Storm of August 15, 1940

The storm developed between 10 and 20 kilometers north of the instrument field about 6:00 p.m. The first thunder from a stroke 16 kilometers distant was heard at

6:14 p.m. and all the recorders were in operation at 6:27 p.m. The storm was well developed but not old at the time the electrical records began. Figure 8 shows the horizontal distribution of charges at 8-minute intervals and figure 9 shows the vertical distribution for the same intervals. Six regions, three negative and three positive, were clearly identified. There is evidence of two other short-lived negative regions that have been left unnumbered. The positive charges lay principally to the west of the negative charges but a few positive charges were also found to the east. All regions moved toward the southeast with an average velocity of 20 kilometers per hour. The negative regions had a mean velocity of 22 kilometers per hour; while the positive regions had a mean velocity of 17 kilometers per hour. Figure 10 shows that paths of the centers are nearly parallel and have the curvature of an anticyclonic wind system.

The negative centers remain nearly 1 kilometer below the positive centers throughout the storm, but the average height of both negative and positive centers decreases nearly 1 kilometer from the first to the last interval. The stroke frequency decreases with time. Ground strokes, which predominate in the early part of the storm, are not observed in the last part of the storm. A few charges appearing in table I and associated with a weak storm west of the one shown were omitted in plotting the diagrams. The strokes were so infrequent that no attempt was made to locate charge regions.

The rain sheets were of moderate intensity and moved in the same direction as the centers with a velocity of about 20 kilometers per hour. Accurate location with respect to the positive and the negative centers was not feasible because of the distance from the observer. It is interesting to note that the average wind velocity in the region between 3.5 and 8.5 kilometers above the surface was 18 kilometers per hour NW at 3:00 p.m. This value is in good agreement with the observed velocity of both rain sheets and charge centers. The angles subtended by the rain sheets were in good agreement with angles subtended by active charge centers.

#### Storm of September 3, 1940

The storm was west of the instrument field and fully developed at 2:50 p.m., when the observations were begun. Recorders were turned on by 3:11 p.m., as the storm was

moving east, north of the instrument field. The cloud base extended at least 20 kilometers in a N-S direction and more than 20 kilometers in an E-W direction. The rain sheet was very extensive but denser portions could be identified and followed.

In figure 11, which shows the horizontal distribution of charges at 6-minute intervals, 16 centers of activity were located. Of these regions, regions 5, 7, 11, 17, and 19 could be traced from 6 to 12 minutes. Of the regions that had longer life, regions 6, 9, 10, and 13 were less active than the rest and were never marked by more than two discharges in any one 6-minute interval. It should be noted that, in the first intervals studied, most of the regions were well defined by frequent strokes. In the later intervals, as the storm intensity was decreasing, only one or two regions were clearly defined. The motion of all the centers was essentially west to east with a mean velocity of 20 kilometers per hour. (See fig. 13.) The average velocity of the negative centers was 24 kilometers per hour; while that of the positive centers was only 16 kilometers per hour. All the positive centers were slower than 22 kilometers per hour and all the negative centers were faster than 20 kilometers per hour. The paths of the centers that could be distinguished longest had the curvature of an anticyclonic wind system, as in the case of the centers in the storm of August 15.

Region 3 is interesting in that, while it was most active, it was fairly extensive and, as its activity diminished, it seemed to be progressively more constricted by the adjacent positive regions. Its behavior indicates a close correlation between its electrical and dynamical importance in the storm.

During the early part of the storm, the positive regions tended to lie behind (relative to storm motion) the negative regions in fairly regular array. In the later part of the storm, the distribution was less regular. Throughout the storm the positive charges were, on the average, about 0.7 kilometer higher than the negative charges. (See fig. 12.) No satisfactory correlation of the charge height and age of charge region could be found because of the complexity of the storm and because of the infrequent lightning activity in the last intervals.

All lightning strokes were within the cloud during the period of observation. The stroke frequency decreased

markedly from the beginning to the end of the period. That the storm was actually dissipating at the end of the period of observation is clearly shown by the fact that no lightning strokes were observed after 3:55 p.m. although the west side of the cloud overlay the instrument field and 15 kilometers of its base in an east-to-west direction were visible. The irregularities of the last part of the storm were doubtless due to the weakening of the updrafts and the resultant slow mixing.

Because the wind observations for 3:00 p.m. of this date stop at 4.5 kilometers above the surface, it is impossible to make very satisfactory comparison with motions of charge regions. All the observed winds higher than the cloud base of the advancing storm are between WNW and WSW, consistent with the direction of storm motion. The wind at 4.5 kilometers, 10 meters per second or 36 kilometers per hour, is much higher than the observed velocity of the charge centers. Because the storm was already approaching at the time of the wind observations, it is probable that subsidence in advance of the storm may have influenced the magnitudes of the wind velocities. The observations on the rate of advance of rain sheets varied from 16 to 24 kilometers per hour, which is in satisfactory agreement with the average of 20 kilometers per hour for the charge centers.

#### Storm of September 10, 1940

The storm developed northeast of the instrument field in the approximate position shown in figure 14 between 4:25 p.m. and 4:30 p.m. The instruments were all operating at 4:42 p.m. The storm was relatively weak and lasted less than 1 hour. No cloud-ground strokes were observed throughout its duration. Only two charge regions, one negative and one positive, were found and these showed no evidence of progressive displacement although the region of the greatest activity and the amount of the activity varied with time. The negative region was at all times west of the positive region. The rain sheets observed in the direction of the charge centers were light at all times. In the first 10 minutes of the storm, the negative charges were on the average, 0.5 kilometer lower than the positive charges. Subsequently, the positive charges dropped to the same elevation and finally to 0.7 kilometer below.

The vertical distribution of the winds at 3:00 p.m. is very illuminating in this storm situation. The winds

in the first kilometer above the surface are strong easterlies; whereas, the winds at high levels are very strong westerlies, increasing with height to 12.5 kilometers above the surface where the velocity reaches 130 kilometers per hour. The same general wind pattern was also shown in the wind observations at 9:00 a.m. and 9:00 p.m. of September 10 and must have existed at the time of the storm. It is at once evident that under the powerful shearing action at high levels, no thunderhead could achieve great elevation and intense storm is not to be expected. Convection penetrating from the lower to the higher levels in the atmosphere would tend to transfer westward momentum upward so that in the region where westerly current is not too strong a column could rise nearly vertically. Above 6 or 7 kilometers, however, marked shearing action would tend to blow the upper portion of the cloud to the east relative to the base.

The tendency of the storm to remain in the same general position under these conditions is not difficult to understand although the situation is inherently unstable.

The storm is of particular importance because of the evidence it supplies on relative positions of charges. With an essentially stationary storm and increasing westerly winds aloft, it follows that those charges carried to greatest heights in the updraft must experience displacement to the east. The storm shows clearly that the positive charges are the ones so displaced.

#### SUMMARY OF RESULTS

The principal results of the experimental-data study may be summarized as follows:

1. The average charge neutralized by a lightning stroke in the storms studied is 24 coulombs. The result is in essential agreement with the previous results reported in reference 5 and with those of McEachron (reference 7), who found 30- and 35-coulomb averages for cloud-ground strokes only.
2. The principal charges drained by lightning strokes are several kilometers above the cloud base, in the region



where the temperatures are between  $-5^{\circ}\text{C}$  and  $-25^{\circ}\text{C}$ . In the storms studied in Albuquerque, the charges were between 4 and 7 kilometers above the surface or approximately 2 to 5 kilometers above the cloud base. These results are in agreement with charge elevations previously reported by the writers. No concentrations of positive charge were found near the base of the cloud, as has been reported by Simpson and his collaborators.

3. The mean vertical separation of positive and negative lightning charges is less than 1 kilometer and their mean horizontal separation is of the order of 3 kilometers. This result indicates that intracloud strokes are, in general, more nearly horizontal than vertical.

4. All cloud-ground strokes studied transported negative charge to ground, in agreement with previous observations of the writers and other recent observations.

5. A study of the distribution of charges shows that it is possible to identify definite regions of charge that persist for intervals from 10 to more than 30 minutes. These regions travel with moving storms and have approximately the same velocity as the heavier rain sheets under the cloud. The heavy rain sheets are usually found in the vicinity of the active charge regions. In the one case when it was possible to compare the average velocity of the charge regions with the average wind velocity at the charge levels in advance of the storm, the two velocities agreed within 10 percent.

6. Evidence supplied by the storm of September 10 shows that the negative charges lie in the region of the updraft and that positive charges are displaced upward and away from the negative charge in this region. Further evidence on this point is found in the storm of August 15. The negative regions are coherent and positive charges are found on both sides of the negative regions. It might be assumed that the more coherent region was associated with the updraft.

7. Cloud-ground strokes are more frequent in the earlier stages of the development of an active region of the thunderstorm. As an active region ages, the lightning strokes become predominantly or exclusively intracloud strokes. The aging is also characteristically associated with a decrease in stroke frequency.

## DISCUSSION OF THUNDERSTORM STRUCTURE

The data presented are consistent with the following suggested thunderstorm pattern. In an active region of a thunderstorm, the charge-generating process occurs in the updraft and is associated with condensation forms of more than one phase. The positive charges are carried upward with respect to the negative charges. Near the top of the air fountain, where the vertical motion of the air is small, the positively charged particles begin descent in the vicinity of, but outside, the main updraft. As suggested by C. T. R. Wilson (reference 1) this action would make the essential polarity of the thunderstorm positive upward. The positive charges, however, do not exist in large concentration in the highest portions of the cloud. Repeated attempts by the writers to detect charge in the thunderstorm anvil that extends well in advance of the main body of the storm have been made with a sensitive generating voltmeter capable of measuring gradients of 0.1 volt per centimeter. No significant change in the gradient has been observed with the anvil overhead until the main storm becomes sufficiently close to allow the charges at about 7 kilometers above the surface to account for the altered gradient.

As positive charges return toward the level of the negative charges, frequent lightning strokes occur between the cloud charges of opposite sign. Since the positive charges are descending from above, the chance that an intracloud stroke will connect a higher positive charge with a lower negative charge is greater than for the reverse situation. In the most vigorous phase of the life of an active region while the updraft is strongest, the positive charges are carried to greater heights and both the horizontal and the vertical separation of the charge are large. Under these circumstances, discharges from the negative region to ground are frequent. As the active region ages, the updraft weakens and the separation of charges is less. In this stage, the intracloud strokes predominate. Some nearly vertical intracloud strokes might be expected in the air fountain and the writers previously have observed some of these in the earliest stages of the storm. The fact that relatively few strokes of this type are observed in a well-developed storm may be due to a continuous variation in the relative concentration of positive and negative charges in the region of charge separation that would result in low gradients above the negative region. Below and to the side of the negative region these conditions would not prevail.

Since all of the observed cloud-ground strokes carry negative charge downward, not all of the positive charge in the active region would be neutralized by intracloud strokes, and the rain that falls in the vicinity of the updraft during its most active period should be positive. Turbulence that exists toward the edge of the updraft should transport some negative charge outward so that the region of negative charge would tend to be larger than the main updraft itself.

Because negative regions are associated with regions of rapid upward vertical motion, examination of the storms on August 15 and September 3 lead to the following interpretations. In any extensive and well-developed storm, several strong updrafts may exist. These regions have a certain dynamical stability, may exist for periods in excess of half an hour, and tend to move with the body of the storm. The relative positions of negative regions indicate that updrafts may have a horizontal separation of less than 4 kilometers. This cellular structure has been evident in delayed-action motion pictures of storms that have been taken by the writers during the past four seasons. Further study of this aspect of structure is contemplated during the next thunderstorm season.

Two observations in complicated storms are of special interest: First, negative regions tend to move more rapidly than positive regions; and, second, more negative than positive regions can be identified. While the data obtained are not adequate to give unique explanation of the observations on exceedingly complicated thunderstorm phenomena, some possible explanations of the phenomena are suggested. The relative horizontal displacement of the positive and the negative regions is probably determined by asymmetries in the complicated wind system within the cloud that produces asymmetries in the air fountain. It may be assumed that in a moving storm the upper part of the cloud tends to suffer some shear with respect to the base in the direction of motion. Ice particles from the top of the fountain would tend to be displaced forward with respect to the main updraft and fall ahead of it. In accordance with the Bergeron-Findeisen theory of precipitation, the ice particles would grow at the expense of supercooled water droplets as they descend toward the base of the cloud because of the difference in saturation vapor pressure of ice and water surfaces at the same temperature below freezing. The liberation of the latent heat of fusion of the supercooled drops would warm the air in advance of the updraft. This

warming would produce a tendency toward instability, especially if the concentration of droplets is greater at the lower levels. If a saturation adiabatic lapse rate existed in the cloud, the process would produce vertical instability and favor the forward development of the region of the updraft. The updraft in developing in a forward direction would have a larger phase velocity than the positive regions of the storm. This explanation of the phase development of the updraft would account for the somewhat irregular behavior of storms that develop in a region where wind velocities are small.

As the ice particles in a precipitation sheet fall into the base of the cloud, below the  $0^{\circ}\text{C}$  isothermal surface, they begin to melt and cool the surrounding air as a result of the extraction of the latent heat of fusion. If an adiabatic lapse rate already existed in the space below the base of the cloud, the cooling at the upper side of this layer of air would produce instability beneath the cloud, the cooling at the upper side of this layer of air would produce instability beneath the cloud. Such a process has previously been suggested as a possible cause of tornadoes under intense storm conditions. In a lesser degree in ordinary thunderstorms, the process may account for the development of new active centers, perhaps at the edge of positively charged regions where subsidence of precipitation forms occurs. Region 5 in the storm of September 3, for example, may have developed in this way. The multiplicity of active centers in a storm may be due to instabilities produced by an original active center by such a process. The storm would then continue to grow until the vertical mixing of the air reduced the storm potential energy to the point where it ceased to exist as a thunderstorm.

Although the results of the study do not lead to a clear-cut theory of the charge-generating process in a cloud, the observations throw some light on the subject. The principal thunderstorm charges are produced in a region of ice forms and supercooled droplets where the temperatures are between  $-5^{\circ}\text{C}$  and  $-25^{\circ}\text{C}$ . It is, therefore, improbable that the original unmodified Simpson breaking-drop theory is a satisfactory explanation of the production and the distribution of the major thunderstorm charges. Simpson and his collaborators have recognized that this is probably the case in the higher thunderstorm charges but present evidence for the existence of a region of positive charge

near the base of thunderstorms, below the  $0^{\circ}\text{C}$  isotherm, where the existence of the breaking drop process seems more probable. No such active region has been found in the current study and the results must be interpreted to mean that, if such a region exists, it does not involve large charges that are frequently drained by lightning strokes. It is, of course, possible that the thunderstorms studied at Kew by Simpson and others are sufficiently different from the Albuquerque storms to account for the difference in observation. The Kew storms had characteristically low bases and the  $0^{\circ}\text{C}$  isotherm was well up in the cloud, so that a relatively large volume of water droplets could exist. The Albuquerque storms, on the other hand, had characteristically higher bases and the  $0^{\circ}\text{C}$  isotherm was much closer to the base of the cloud. Granting that some differences in storm conditions exist and also that the breaking-drop process can and probably does exist in some regions of the thundercloud, it seems doubtful that this process is the fundamental cause of the production of the major thunderstorm charges.

Some other observations made in the course of the study are of incidental interest. The observation that all cloud-ground strokes transported negative charge to ground suggests that during appreciable intervals of the life of a thunderstorm the net-thunderstorm charge is positive. This fact suggests that the Wilson induction theory of charge production may explain part of the observed thunderstorm phenomena. Furthermore, this fact, may well account for the observations at Kew Observatory that the rain from thunderstorms carries a net positive charge. It also lends support to the theory that thunderstorms, which are continuously in progress in some region of the earth, are responsible for the negative charge of the earth. If, in every thunderstorm, only the negative charges were carried to earth by lightning and the positive charges more gradually returned by rain, the negative charge on the earth at any one time should be approximately equal to the sum of the net positive thundercharges of the storms then in progress.

Another point of meteorological interest is the anticyclonic curvature of the paths of the thunderstorm charge regions. It is a well-known result in dynamic meteorology that, when winds blow over mountain ranges, a region of high pressure is produced on the windward side and a region of low pressure on the lee side of the mountains. As a

result of the creation of the pressure ridge and trough, the winds tend to curve anticyclonically on the windward side and cyclonically on the lee side of the mountain range. In the storms of both August 15 and September 3, the winds had a W component blowing the storms toward the Sandia range east of the field. The curvature first became evident about 10 kilometers west of the base of the mountains and 15 kilometers west of the ridge. The storm speeds of both days were about 20 kilometers per hour although on August 15 the prevailing winds at thunderstorm levels were from northwest while on September 3 they were from the west. The observation indicates that, while the thunderstorm may be a major local disturbance of the wind pattern, its general motion is governed approximately by the prevailing winds if they are strong and essentially in the same direction at all levels.

The thunderstorm of September 10 did not follow the strong upper winds but the wind pattern in the lower levels was quite different from the usual thunderstorm within a single air mass as noted previously.

#### REMARKS ON DISTRIBUTION OF GRADIENTS WITHIN

##### A STORM AND AIRCRAFT SAFETY

While it is evident that in a complicated storm condition the detailed prediction of the distribution of gradients is impossible, the data on charge location just described make possible estimates of the order of magnitude of the gradients and the approximate regions in which the gradients are greatest and in which the gradients are changing most rapidly.

Not all of the charges that are shown in the charge-distribution diagrams exist simultaneously in a storm. The interval between successive large lightning strokes is of the order of a minute or more and two large strokes usually do not occur in the same vicinity within an interval of several minutes. It was assumed, therefore, that a single dipole with a charge magnitude somewhat above the average observed would serve as a satisfactory basis for estimating the order of magnitude of the gradient distributions within the body of the storm at any one instant.

Four vertical sections of a storm were prepared to show the distribution of gradients for 33-coulomb charges if no other cloud charges or space charges existed in the storm. Figure 15 shows the distribution of vertical gradients for: (a) a single 33-coulomb charge at 5 kilometers above the surface; (b) two 33-coulomb charges of opposite sign at 5 and 6 kilometers above the surface, respectively, and with a horizontal separation of 3 kilometers. The two remaining diagrams (fig. 16) show the horizontal gradient distribution for the same charges. The single-charge pattern represents approximate conditions if one charge is at considerable distance from others, and the dipole pattern represents a characteristic situation as found in the storms studied. The continuous curves connect points with equal horizontal or vertical gradients and the numerical values are in volts per centimeter.

Inspection of the diagrams shows that the maximum vertical gradients exist immediately above and below the charge concentrations, and the maximum horizontal gradients exist at the same level as the charges. If a thunderstorm volume of 1000 cubic kilometers and the dipole shown in figures 15 (b) and 16 (b) are assumed, the region in which vertical (or horizontal) gradients of 100 volts per centimeter or more would exist would be less than 25 percent of the cloud volume. The region in which vertical gradients of more than 300 volts per centimeter would exist is less than 10 percent of the total volume.

If the charges shown in the figures were surrounded by space-charge envelopes, the gradients everywhere outside the envelopes would be decreased. For example, if spherical symmetry is assumed and if a space-charge envelope contained a charge equal to one-half the cloud charge, the gradients outside the envelope would be reduced to 50 percent of the values shown. It should be noted, however, that if a large space-charge is assumed the gradients produced by the space charges themselves after a lightning stroke occurs would be opposite in sign to those existing before the stroke. In the case just cited, with a space charge equal to one-half the cloud charge, immediately after a stroke the gradients would have the same magnitude but would be oppositely directed. The larger the assumed space charge, the larger the gradients after the stroke. It may, therefore, be concluded that even if an appreciable space charge around the cloud charges is assumed, gradients of the order of magnitude shown will exist at some time either preceding or following the lightning discharge.

It is obviously impossible to predict in detail what other cloud charges may exist simultaneously with the charges shown in the diagrams. It seems unlikely, however, that the existing gradients will be of a different order of magnitude.

Simpson and Scrase (reference 2) and Simpson and Robinson (reference 3) claim that they did not observe vertical gradients greater than 100 volts per centimeter in most of their soundings in thunderstorms. They further pointed out that the vertical gradient did not change rapidly with height beneath the cloud. Considering the last-mentioned point first, it should be noted that rapid variation of vertical gradient with height near the surface would not be expected, even if no space charge were assumed. With the charge distributions chosen, the vertical gradient is nearly constant under the cloud base except directly under the charges where they may increase by a factor of two as the cloud base is approached. With respect to the order of magnitude of the gradients observed, Simpson and his collaborators emphasize that their vertical-gradient recorder, the alti-electrograph, is reliable with respect to sign of the gradient but indicates only correct orders of magnitude and not precise quantitative results. With this fact in mind and recognizing that, on any simple assumption, large gradients are not to be expected except in small thunderstorm volumes at any one time, the suggested distribution of gradients previously discussed are not necessarily in disagreement with the alti-electrograph records.

One of the principal dangers to aircraft in thunderstorms is the chance that the craft may become part of a lightning channel. Even with all-metal airplanes where the structural damage due to lightning is reduced to a minimum, the danger of visual or aural shock to the pilot and of damage to the instruments remains. Two cases of lightning strokes to airplanes may be distinguished: (1) The airplane becomes part of a channel that originates at some distance away; (2) The airplane becomes part of a channel that the airplane itself may have originated.

In consideration of the first case, it may be noted that present theories of lightning propagation indicate that lightning strokes in particular, leader strokes propagate themselves as a result of processes occurring near the tip of the leader. Thus, if the airplane is far from the region of large charges where the lightning channel originated, it would not become part of the stroke unless it were, by chance, within a distance of the channel of the order of magnitude of



the linear dimensions of the airplane itself. On this assumption a transport airplane flying at normal cruising speed under the storm of August 15 at the height of its activity would have less than one chance in a thousand of being struck.

The second case would occur in the vicinity of the charge concentrations that ordinarily are drained by lightning strokes. In the high electric fields in the vicinity of these charges the airplane would develop corona discharges from parts of its structure with high curvature. The corona might well develop into a leader stroke, thus making the airplane a part of the stroke that it aided in originating. The probability of this occurrence cannot be readily estimated. It clearly would be greatest in the regions where large charge concentrations are developing and in these regions, doubtless, it would be more probable than would be the chance of a lightning strike due to the first cause described.

As a result of these considerations, it appears that the maximum danger of lightning strokes to airplanes is in that region where the potential gradients are greatest and are changing most rapidly with plane displacement. Figures 15 (b) and 16 (b) show that these regions are most likely to occur where the temperature is between  $-5^{\circ}\text{C}$  and  $-25^{\circ}\text{C}$ . Since it is not, in general, feasible to fly over these regions unless an airplane is equipped with oxygen or a pressure cabin, the safest procedure (if flying through a storm region is inevitable) is to fly as low as the character of the terrain permits. It is generally safer to fly below the cloud base away from regions where the rain sheet is heaviest and cloud-ground strokes are most frequent. If flying through the cloud is necessary, flying below the level of the  $0^{\circ}\text{C}$  isothermal surface is indicated.

It is of interest to note that radio static due to corona discharge will be a minimum in those regions just noted in which flight is safest.

### CONCLUSIONS

From the time histories of thunderstorm charge distribution during three storms occurring in the summer of 1940 in the vicinity of the Albuquerque airport obtained

from eight synchronized recording electrometers arranged in a particular pattern over a field 1.6 kilometers above sea level, it has been concluded:

1. The method of obtaining and analyzing electrical data described is adequate to determine the sign, the magnitude, and the position of the electric charge or charges associated with each stroke.

2. The average charge neutralized was 6.5 coulombs per stroke element and 24 coulombs for a complete lightning stroke.

3. The weighted average height of the negative charges was 5.2 kilometers and of the positive charges was 5.8 kilometers above the surface; that is, the mean vertical separation of charges was less than 1 kilometer. The heights actually ranged between 4 and 7 kilometers and included the region where the temperature is between  $-5^{\circ}\text{C}$  and  $-25^{\circ}\text{C}$ .

4. Horizontal separations between charges involved in an intracloud stroke varied between 1 and 10 kilometers. The weighted mean value was 3 kilometers.

5. Cloud-ground strokes were observed only on August 15, and all of these strokes transported negative charges to the ground. This result is in agreement with those of previously reported observations.

6. A study of the distribution of charges showed that it was possible to identify definite regions of charge that persisted for intervals from 10 to more than 30 minutes. These regions traveled with moving storms and had approximately the same velocity as the heavier rain sheets. In the one case when it was possible to compare the average velocity of the charge regions with the average wind velocity at the charge levels in advance of the storm, the two velocities agreed within 10 percent.

7. Evidence supplied by the storm of September 10 showed that the negative charges were in the region of the updraft and that positive charges were displaced upward and away from the negative charge in this region. Further evidence was found in the storm of August 15. The negative regions were coherent and positive charges were found on both sides of the negative regions. The evidence is consistent with the hypothesis that the more coherent region was associated with the updraft.

8. Cloud-ground strokes were more frequent in the earlier stages of the development of an active region of the thunderstorm. As an active region aged, the lightning strokes became predominantly or exclusively intracloud strokes. The aging was also characteristically associated with a decrease in stroke frequency.

9. The maximum vertical potential gradients existed immediately above and below the charge concentrations, and the maximum horizontal gradients existed at the same level as the charges.

10. One of the principal dangers to aircraft in thunderstorms is the possibility that the craft may become part of a lightning channel. This possibility is greatest in regions where the potential gradients are greatest. The present investigation showed that these regions are most likely to occur where the temperature is between  $-5^{\circ}\text{C}$  and  $-25^{\circ}\text{C}$ .

University of New Mexico

Albuquerque, New Mexico, May 6, 1942.

## REFERENCES

1. Wilson, C. T. R.: Some Thundercloud Problems. Jour. Franklin Inst., vol. 208, no. 1, July 1929, pp. 1-12.
2. Simpson, George, and Scrase, F. J.: The Distribution of Electricity in Thunderclouds. Proc. Roy. Soc., London, ser. A, vol. 161, no. 906, Aug. 3, 1937, pp. 309-352.
3. Simpson, George, and Robinson, G. D.: The Distribution of Electricity in Thunderclouds, II. Proc. Roy. Soc., London, ser. A, vol. 177, no. 970, Feb. 24, 1941, pp. 281-329.
4. Minser, E. J.: Meteorological Conditions Associated with Aircraft Lightning Discharges and Atmospherics. Jour. Aero. Sci, vol. 7, no. 2, Dec. 1939, pp. 51-55.
5. Workman, E. J., and Holzer, R. E.: A Preliminary Investigation of the Electrical Structure of Thunderstorms. T. N. No. 850, NACA, 1942.
6. Macky, W. A.: Some Investigations in the Deformation and Breaking of Water Drops in Strong Electric Fields. Proc. Roy. Soc., London, ser. A, vol. 133, no. A 822, Oct. 1, 1931, pp. 565-587.
7. McEachron, K. B.: Lightning to the Empire State Building. Jour. Franklin Inst., vol. 227, no. 2, Feb. 1939, pp. 149-217.

TABLE I

STORM OF AUGUST 15, 1940 - SUMMARY OF CHARGE ANALYSIS

Time (hr:min:sec) (a)	Type of stroke (b)	Charge coordinates			Q magnitude of charge
		x	y	z	
6:28:21a	G	6.6	6.2	-6.5	4
:28:21b	G	5.2	6.3	-5.5	5
:28:21c	G	6.1	5.7	-6.5	4
:28:21d	G	5.7	6.5	-6.5	6
:28:21e	G	0.5	9.0	-6.0	2.5
:28:55a	C	4.5	2.5	7.0	1.5
		5.6	7.2	-5.5	
:28:55b	C	9.5	3.0	6.5	2
		5.7	2.5	-6.0	
:30:14a	C	1.3	-0.8	7.0	2.5
		7.4	2.0	-6.0	
:30:14b	C	9.0	4.9	6.0	10
		6.7	4.5	-5.0	
:30:14c	C	4.4	2.5	7.0	2.5
		6.0	3.3	-6.0	
:31:25a	G	5.9	6.2	-5.5	12
:31:25c	G	6.7	6.2	-6.0	5
:31:25d	G	7.3	5.3	-5.0	12
:33:49a	G	5.8	4.4	-5.0	6
:33:49b	G	6.6	5.6	-6.0	5
:33:49c	G	5.3	6.5	-6.0	6
:33:49d	G	5.0	5.0	-6.0	4
:35:13a	G	6.3	4.8	-5.0	6
:35:13c	C	4.3	4.3	7.0	12
		5.0	6.2	-6.0	
:35:46a	G	6.4	3.7	-7.0	5
:36:30a	C	0.9	0.0	7.0	1
		7.5	0.8	-6.0	
:36:30b	G	5.1	2.7	-4.0	4
:37:44c	G	7.2	5.3	-4.5	4
:39:48a	C	4.0	4.5	7.0	10
		6.8	5.8	-6.0	
:39:48b	C	6.9	7.2	7.0	3
		4.8	5.6	-6.0	
:40:18a	C	5.0	-0.3	7.0	6
		5.4	0.7	-6.0	
:40:18b	C	4.3	1.9	6.0	1
		4.9	4.4	-5.0	

See footnotes at end of table.

TABLE I (Continued)

STORM OF AUGUST 15, 1940 - SUMMARY OF CHARGE ANALYSIS

Time (hr:min:sec) (a)	Type of stroke (b)	Charge coordinates			Q magnitude of charge
		x	y	z	
6:40:18c	C	-2.7	8.3	6.0	2
		5.2	4.1	-5.0	
:40:38a	C	-11.4	3.0	7.0	8
		6.5	6.0	4.5	
:41:13a	C	5.3	3.2	7.0	8
		9.3	2.3	-5.0	
:41:13b	C	2.2	4.3	7.0	5
		2.1	7.0	-6.0	
:41:13c	C	3.8	2.8	7.0	2
		3.7	6.1	-6.0	
:41:52a	C	4.7	-0.3	5.5	4.8
		8.4	-1.5	-4.5	
:42:13a	C	3.0	6.0	6.0	10
		4.0	7.9	-5.0	
:42:36a	C	-7.2	5.4	6.0	10
		5.0	3.7	-5.0	
:43:18b	C	4.3	3.1	7.0	5
		5.1	6.3	-6.0	
:44:11a	C	4.0	6.8	6.0	25
		5.0	7.7	-5.0	
:44:11b	C	6.8	0.5	6.0	5
		9.2	2.6	-5.0	
:45:35a	C	5.8	4.6	7.0	15
		7.2	6.3	-6.0	
:45:35b	C	5.5	2.3	7.0	6
		9.3	3.2	-6.0	
:46:26a	C	-6.3	4.0	6.0	8
		-8.0	4.6	-5.0	
:46:26b	C	-3.2	2.6	6.0	4
		-7.3	5.6	-6.0	
:46:26c	C	-4.7	2.7	6.0	6
		-9.5	1.6	-5.5	
:46:46a	G	8.8	5.0	-5.0	2
:46:46b	G	8.5	1.8	-5.0	1
:46:46d	G	9.3	3.2	-5.0	.25
:48:20a	G	8.6	1.4	-6.0	1
:48:20b	G	7.3	5.0	-5.0	1
:48:20c	G	6.9	1.2	-6.0	.3

See footnotes at end of table.

TABLE I (Continued)

## STORM OF AUGUST 15, 1940 - SUMMARY OF CHARGE ANALYSIS

Time (hr:min:sec) (a)	Type of stroke (b)	Charge coordinates			Q magnitude of charge
		x	y	z	
6:48:20d	G	8.4	2.9	-6.0	1
:48:20e	C	5.8	0.5	7.0	2
		4.8	1.1	-6.0	
:48:20f	G	6.6	2.7	-5.0	4
:49:02a	C	5.5	1.1	6.0	12
		4.7	-0.6	-5.0	
:49:39b	G	13.0	1.6	-4.5	1
:50:05a	C	6.8	4.5	6.0	25
		8.0	5.3	-5.0	
:55:05a	C	7.7	0.7	6.0	10
		9.8	-1.6	-5.0	
:55:05b	C	5.8	3.3	6.0	5
		8.8	3.9	-5.0	
:57:18b	C	8.8	4.6	6.0	7
		7.7	2.1	-5.0	
:59:41a	C	-1.0	7.6	5.0	90
		1.1	8.9	-4.0	
7:01:36a	C	-0.1	2.0	3.5	20
		0.7	2.0	-3.0	
:02:20a	C	7.0	3.7	5.5	30
		7.4	5.2	-4.5	
:05:47a	C	6.3	0.4	6.0	8
		9.5	0.6	-5.5	
:05:47b		7.3	1.1	5.0	6
		9.7	0.2	-4.0	
:05:47c	C	9.4	0.0	6.0	11
		10.4	0.4	-5.0	
:09:26b	C	9.5	0.2	6.0	33
		10.0	-0.7	-5.0	
:13:27a	C	-3.4	9.4	6.0	4
		-4.2	4.0	-5.0	
:13:27b	C	2.7	8.5	6.0	15
		2.8	8.6	-5.0	

(a) Letters indicate particular stroke elements

(b) G, cloud-to-ground stroke

C, cloud-to-cloud stroke

TABLE II

## STORM OF SEPTEMBER 3, 1940 - SUMMARY OF CHARGE ANALYSIS

Time (hr:min:sec) (a)	Type of stroke (b)	Charge coordinates			Q magnitude of charge
		x	y	z	
3:11:25a	C	-1.7	10.3	5.0	5
		-1.4	5.9	-5.0	
:11:25b	C	-4.1	9.0	5.0	6
		-3.4	6.9	-6.0	
:15:03a	C	-2.3	-4.5	5.0	5
		4.2	-9.0	-5.5	
:15:03b	C	-2.8	-6.0	5.0	25
		-2.5	-3.5	-5.0	
:15:03c	C	-4.2	-4.4	5.0	33
		-4.8	-8.0	-5.0	
:15:03d	C	1.6	6.2	6.0	8
		4.7	8.8	-5.5	
:15:03f	C	1.0	9.0	5.5	12.5
		-2.8	4.5	-4.5	
:15:10a	C	-1.8	6.8	5.0	5
		-2.1	6.9	-5.0	
:15:10b	C	-5.4	4.7	5.0	2
		-5.9	2.5	-6.0	
:16:26b	C	-6.8	7.0	5.0	5
		-5.9	5.9	-6.0	
:16:26c	C	-8.4	4.8	7.0	7
		-7.0	3.7	-7.0	
:16:59a	C	0.8	6.0	5.0	31
		1.9	8.2	-5.0	
:16:59b	C	-1.9	6.2	5.0	15
		-3.8	4.3	-4.5	
:17:45a	C	-0.8	8.0	5.0	2
		-4.0	4.0	-6.0	
:17:45b	C	-7.9	5.0	5.0	30
		-6.7	4.3	-6.0	
:17:45c	C	-4.0	7.0	6.0	5
		-2.0	4.0	-4.0	
:18:51a	C	-5.0	5.0	6.0	5
		-1.2	3.8	-5.5	
:18:51b	C	0.0	-4.5	5.0	13
		-3.8	-4.2	-5.0	

See footnotes at end of table



TABLE II (Continued)

## STORM OF SEPTEMBER 3, 1940 - SUMMARY OF CHARGE ANALYSIS

Time (hr:min:sec) (a)	Type of stroke (b)	Charge coordinates			Q magnitude of charge
		x	y	z	
3:19:00a	C	2.3	6.2	5.0	2.5
		4.2	7.3	-6.5	
:19:00b	C	3.1	6.4	5.0	4
		5.0	6.8	-5.0	
:19:00c	C	0.0	5.0	5.5	12
		5.0	5.0	-5.5	
:19:56a	C	-0.7	4.7	5.0	1
		-6.6	7.1	-5.5	
:21:42a	C	-4.5	4.5	6.0	2
		-8.5	2.5	-4.5	
:21:42b	C	2.9	4.8	5.0	6
		6.9	4.3	-5.0	
:22:12a	C	-9.8	2.4	5.0	6
		-8.1	2.1	-7.0	
:23:29a	C	1.1	3.3	5.5	11
		8.3	4.8	-6.0	
:23:49a	C	-6.0	7.3	6.0	8
		-3.6	4.0	-4.5	
:23:49b	C	0.4	8.2	6.0	27
		-1.0	4.3	-4.5	
:24:48a	C	-5.4	5.6	6.0	12
		-6.0	7.9	-5.0	
:25:35b	C	-1.1	7.3	5.0	5
		-2.5	9.0	-5.0	
:26:07a	C	1.0	8.1	5.5	4
		0.5	9.9	-5.0	
:27:01a	C	0.8	5.3	5.0	1.5
		1.6	7.8	-5.0	
:27:29a	C	3.3	3.5	6.0	1
		1.8	2.8	-5.0	
:27:29b	C	3.0	3.0	6.0	1
		2.0	2.6	-5.0	
:28:01a	C	-6.7	3.3	6.5	8
		-7.8	4.8	-5.0	
:28:01b	C	-5.3	5.7	5.0	15
		-8.7	4.8	-5.0	
:28:36a	C	3.8	6.7	6.0	100
		1.6	9.8	-5.0	

See footnotes at end of table

TABLE II (Continued)

## STORM OF SEPTEMBER 3, 1940 - SUMMARY OF CHARGE ANALYSIS

Time (hr:min:sec) (a)	Type of stroke (b)	Charge coordinates			Q magnitudes of charge
		x	y	z	
3:29:49a	C	4.0 3.0	7.5 6.0	6.0 -5.0	1
:31:14a	C	3.0 6.7	3.7 3.7	6.0 -4.5	50
:31:26b	C	-6.1 -8.0	1.9 4.2	6.0 -5.0	8
:31:33a	C	5.2 3.5	6.7 4.3	6.0 -6.0	1
:32:21a	C	2.9 6.5	2.2 1.3	6.5 -6.5	2
:35:21a	C	-1.0 -1.0	6.0 8.5	6.0 -6.0	1.5
:35:21b	C	0.8 -6.0	7.5 9.5	7.0 -5.0	5
:36:18a	C	1.0 -1.5	5.7 9.0	6.0 -5.5	3.5
:38:31a	C	-2.0 -3.5	4.0 5.5	5.5 -5.0	75
:40:34a	C	-5.0 -7.3	4.5 4.5	7.0 -4.5	100
:41:48a	C	-2.5 -6.2	4.2 4.9	5.5 -5.0	30
:44:10a	C	2.2 6.2	5.0 5.8	5.0 -7.0	20
:45:00a	C	-2.0 -0.8	3.7 9.8	6.5 -5.5	2
:45:00b	C	-2.8 -2.3	5.5 10.2	5.5 -5.0	10
:47:06a	C	-2.5 -2.8	8.0 9.5	6.0 -5.0	15
:47:06b	C	3.2 8.5	4.7 3.5	5.5 5.0	25
:50:04a	C	-1.0 -0.5	5.0 7.0	5.5 -5.0	15
:54:38a	C	-0.6 -0.8	5.6 8.0	5.5 -5.0	23

(a) Letters indicate particular stroke elements

(b) G, cloud-to-ground stroke

C, cloud-to-cloud stroke

TABLE III

## STORM OF SEPTEMBER 10, 1940 - SUMMARY OF CHARGE ANALYSIS

Time (hr:min:sec) (a)	Type of stroke (b)	Charge coordinates			Q magnitude of charge
		x	y	z	
4:43:47a	C	6.8	4.5	6.0	1
		6.0	2.8	-6.5	
:43:47b	C	6.0	2.6	6.0	20
		6.2	4.5	-6.0	
:44:15a	C	7.0	5.1	6.0	15
		4.7	4.1	-5.5	
:45:29a	C	6.7	6.0	6.5	1
		4.8	2.8	-6.0	
:45:29b	C	4.4	7.9	6.5	1
		4.3	5.3	-6.0	
:45:29c	C	7.4	6.1	6.5	1
		5.7	3.8	-6.5	
:45:29d	C	7.4	6.1	6.5	1
		4.4	3.5	-6.5	
:45:51a	C	-6.5	-2.0	5.5	23
		-9.7	-2.2	-4.5	
:46:13a	C	-4.4	-3.7	7.0	1.5
		-6.4	-5.6	-5.5	
:46:13b	C	9.3	0.0	6.5	4
		5.0	4.0	-6.0	
:48:05a	C	6.1	5.1	6.5	1
		4.6	4.0	-5.5	
:48:05b	C	7.9	2.9	6.5	1
		5.7	1.8	-6.0	
:48:05c	C	7.5	4.2	6.5	1
		4.5	1.7	-6.0	
:50:07a	C	7.2	7.7	6.5	1
		4.9	2.1	-7.0	
:50:07b	C	9.2	0.5	5.5	2
		6.0	1.0	-6.0	
:50:07c	C	5.8	7.8	5.5	2
		4.5	2.1	-6.0	
:50:07d	C	5.3	9.0	5.5	4
		4.7	2.3	-6.0	
:50:07e	C	7.1	7.8	5.5	4
		4.4	2.1	-6.0	
:50:07f	C	6.1	7.2	5.5	8
		2.2	2.7	-6.0	

See footnotes at end of table.

TABLE III (Continued)

## STORM OF SEPTEMBER 10, 1940 - SUMMARY OF CHARGE ANALYSIS

Time (hr:min:sec) (a)	Type of stroke (b)	Charge coordinates			Q magnitude of charge
		x	y	z	
4:50:07g	C	2.0	8.5	5.0	7
		2.7	3.6	-6.0	
:50:07h	C	4.5	8.4	5.0	7
		1.7	4.7	-7.0	
:50:07i	C	3.9	10.0	5.0	4
		1.8	7.2	-6.5	
:50:07j	C	3.7	10.3	5.0	2
		0.4	8.1	-6.5	
:52:12a	C	4.4	6.9	5.0	2
		4.2	3.0	-6.5	
:52:12b	C	10.1	0.0	6.5	1
		6.3	0.3	-6.5	
:52:12f	C	9.2	4.0	6.5	2
		5.3	2.1	-6.5	
:52:12g	C	10.2	1.4	6.0	4
		5.6	2.0	-6.0	
:52:12h	C	9.7	2.7	6.0	4
		6.3	1.2	-5.5	
:52:12i	C	8.6	0.0	6.0	9
		4.8	1.3	-6.0	
:52:12j	C	-3.0	5.0	5.5	2
		-1.5	3.0	-6.5	
:52:12k	C	3.1	6.1	5.5	4
		2.3	4.4	-6.0	
:55:19a	C	6.2	3.3	5.5	2
		4.7	2.8	-6.5	
:55:19b	C	6.8	6.3	5.5	2
		4.0	4.5	-6.0	
:55:19c	C	4.2	6.6	5.0	2
		3.4	3.4	-6.5	
:55:19d	C	4.0	7.2	5.0	2
		4.2	5.1	-6.5	
:55:19e	C	5.3	6.9	5.5	2
		5.1	4.8	-6.5	
:55:19f	C	5.5	6.1	5.5	2
		4.5	3.6	-6.5	
:55:19g	C	5.9	4.8	6.5	4
		4.4	2.4	-6.5	

See footnotes at end of table.

TABLE III (Continued)

## STORM OF SEPTEMBER 10, 1940 - SUMMARY OF CHARGE ANALYSIS

Time (hr:min:sec) (a)	Type of stroke (b)	Charge coordinates			Q magnitude of charge
		x	y	z	
4:55:19h	C	7.0	4.0	7.0	4
		5.7	2.5	-6.5	
:55:19i	C	8.4	5.0	6.0	40
		5.8	2.3	-6.5	
:55:19j	C	4.6	7.0	5.5	20
		3.5	7.0	-6.5	
:55:19k	C	4.0	5.0	6.5	4
		3.0	3.0	-6.0	
:55:19l	C	6.1	4.0	6.5	2
		2.1	4.3	-6.0	
:55:19m	C	5.5	4.5	6.5	2
		2.5	4.0	-6.0	
:55:19n	C	3.9	6.3	6.5	2
		0.3	5.2	-6.0	
:56:02a	C	5.7	3.7	6.0	1.5
		4.8	2.6	-6.0	
:56:02b	C	6.3	6.5	6.0	1.5
		5.2	3.5	-6.0	
:56:02c	C	4.5	5.8	6.0	1.5
		4.0	3.5	-6.0	
:56:02d	C	3.8	6.0	6.5	1.5
		3.5	3.0	-6.0	
:57:41a	C	8.3	1.8	5.5	8
		5.6	0.5	-6.5	
:57:41b	C	8.3	4.3	6.0	5
		5.8	2.4	-6.5	
:57:41c	C	7.8	6.3	5.5	5
		5.2	3.0	-6.5	
:57:41d	C	8.3	4.8	6.0	5
		4.6	3.2	-6.0	
:57:41e	C	5.2	8.3	5.5	5
		3.8	4.1	-6.5	
:57:41f	C	-3.0	6.0	6.0	2
		-1.0	4.4	-5.5	
:57:41g	C	-3.8	-2.8	5.5	7
		-9.3	-4.8	-5.5	

See footnotes at end of table.

TABLE III (Continued)

STORM OR SEPTEMBER 10, 1940 - SUMMARY OF CHARGE ANALYSIS

Time (hr:min:sec) (a)	Type of stroke (b)	Charge coordinates			Q magnitude of charge
		x	y	z	
5:01:51a	C	7.8	4.9	5.5	2
		5.0	2.0	-6.5	
:01:51b	C	9.2	3.2	5.5	10
		5.5	1.2	-6.0	
:01:51c	C	5.4	7.5	5.5	1.5
		3.2	2.4	-6.0	
:01:51d	C	7.6	5.3	5.5	10
		5.0	3.3	-6.0	
:01:51e	C	8.4	6.3	5.0	.3
		3.8	2.7	-5.5	
:01:51f	C	3.9	8.6	5.0	.3
		3.1	4.2	-5.5	
:01:51g	C	0.9	10.3	5.0	.7
		3.8	3.7	-5.0	
:03:22a	C	7.8	6.2	5.5	2
		4.5	2.9	-6.5	
:04:17a	C	5.2	9.5	4.5	3
		4.8	3.6	-7.0	

(a) Letters indicate particular stroke elements

(b) G, cloud-to-ground stroke.

C, cloud-to-cloud stroke.

TABLE IV

## HEIGHTS OF ISOTHERMAL SURFACES AND CLOUD BASES

Storm	August 15		September 3		September 10	
	Temperature (°C)	Elevation (km)	Temperature (°C)	Elevation (km)	Temperature (°C)	Elevation (km)
Surface	29.4	0	23.9	0	17.2	0
Cloud Base	4.2	2.4	5.7	1.75	9.8	1.4
	0	3.2	0	2.7	0	3.3
	-5	4.05	-5	3.65	-5	4.15
	-10	4.8	-10	4.4	-10	4.95
	-15	5.5	-15	5.2	-15	5.7
	-20	6.2	-20	5.95	-20	6.4
	-25	6.9	-25	6.7	-25	7.1

TABLE V

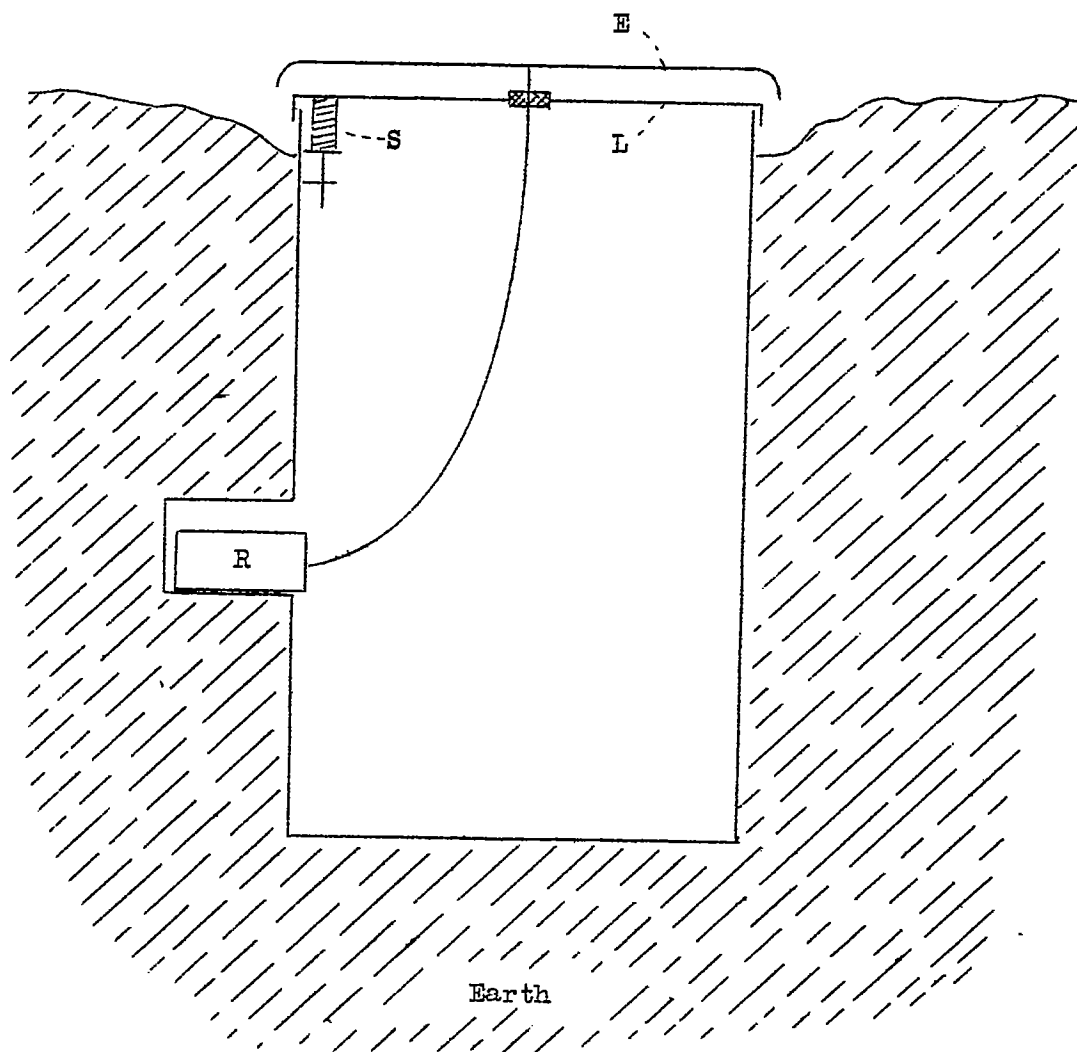
## CHARGE HEIGHTS AND CLOUD TEMPERATURES

Storm	Mean height positive charge (km)	Mean height negative charge (km)	Temperature range in charge region (4-7 km)
August 15	5.8	5.0	-5° to -25°C
September 3	5.7	5.0	-7° to -27°C
September 10	5.7	6.2	-4° to -24°C

TABLE VI  
WIND VELOCITIES AND DIRECTIONS AT 3:00 p.m.

Height (km)	August 15		September 3		September 10	
	Velocity (m/sec)	Direc- tion	Velocity (m/sec)	Direc- tion	Velocity (m/sec)	Direc- tion
0.0	03	SW	03	WNW	11	ESE
.5	04	W	03	NNW	11	ESE
1.0	04	WNW	02	W	06	SE
1.5	06	NW	05	WNW	04	WSW
2.5	03	NNE	05	WNW	05	W
3.5	03	N	07	WSW	08	W
4.5	06	NNW	10	WSW	07	NW
5.5	05	NNE			10	WNW
6.5	03	W			11	W
7.5	07	W			19	W
8.5	11	NW			22	W
9.5	14	WNW			26	W
10.5	16	NW			26	W
11.5	06	NNW			32	W
12.5	07	NW			36	W
13.5	09	NNE			20	W
14.5	08	N				





- E Electrode
- L Lid
- R Recording apparatus
- S Pivot for L (vertical shaft)

Figure 1.- Typical field-apparatus installation.

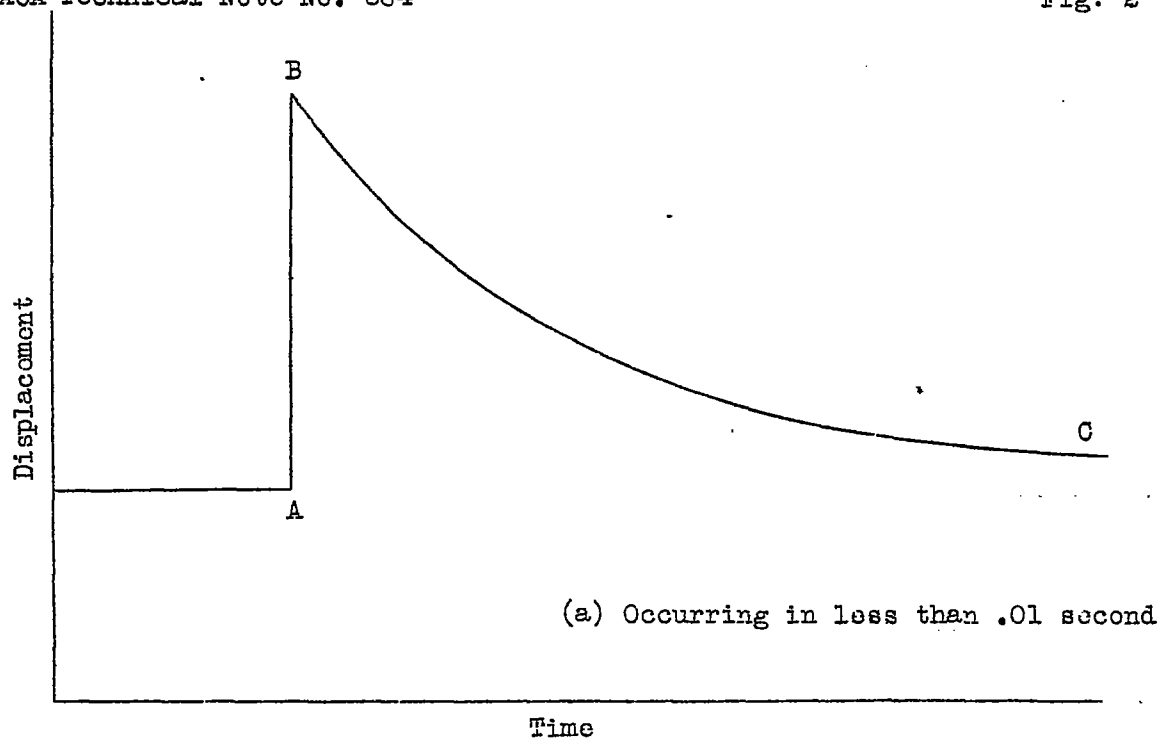
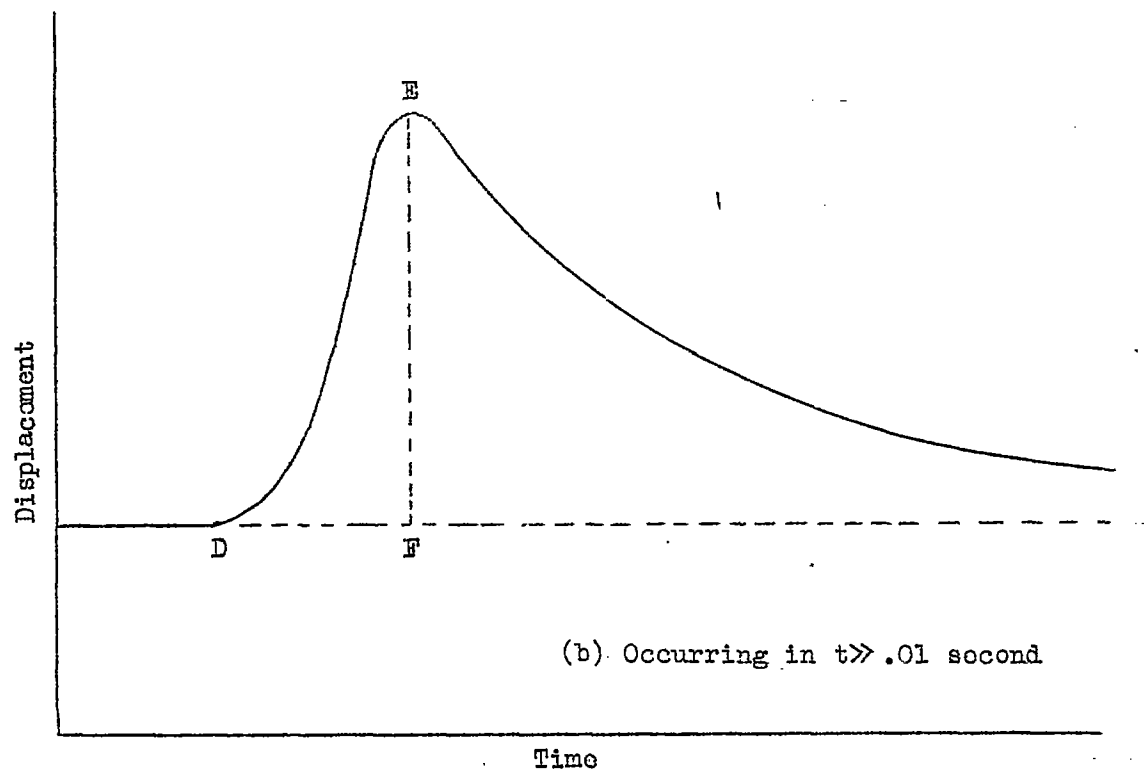


Figure 2.- Responses of recording apparatus to potential-gradient changes.



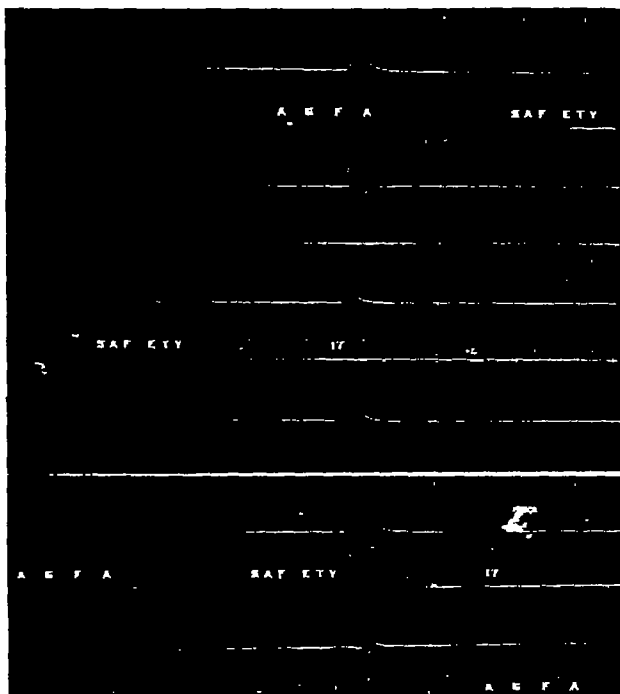


Figure 3.- Contact prints of original film records for characteristic gradient changes occurring during lightning strokes.



Figure 6.- Three convex surfaces for 100-coulomb charges at altitudes of 3, 4, and 5 kilometers.

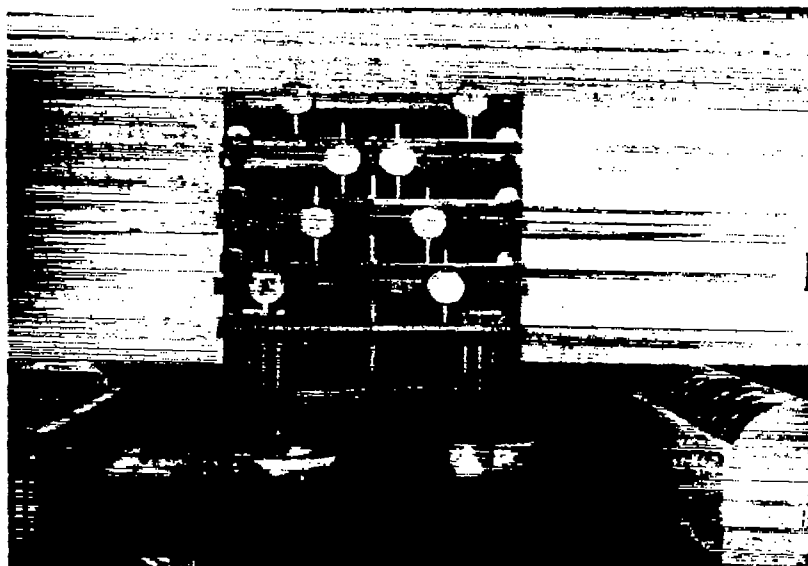


Figure 4.- Analyzer for determining charge structure producing any given set of gradients at the recording instruments.

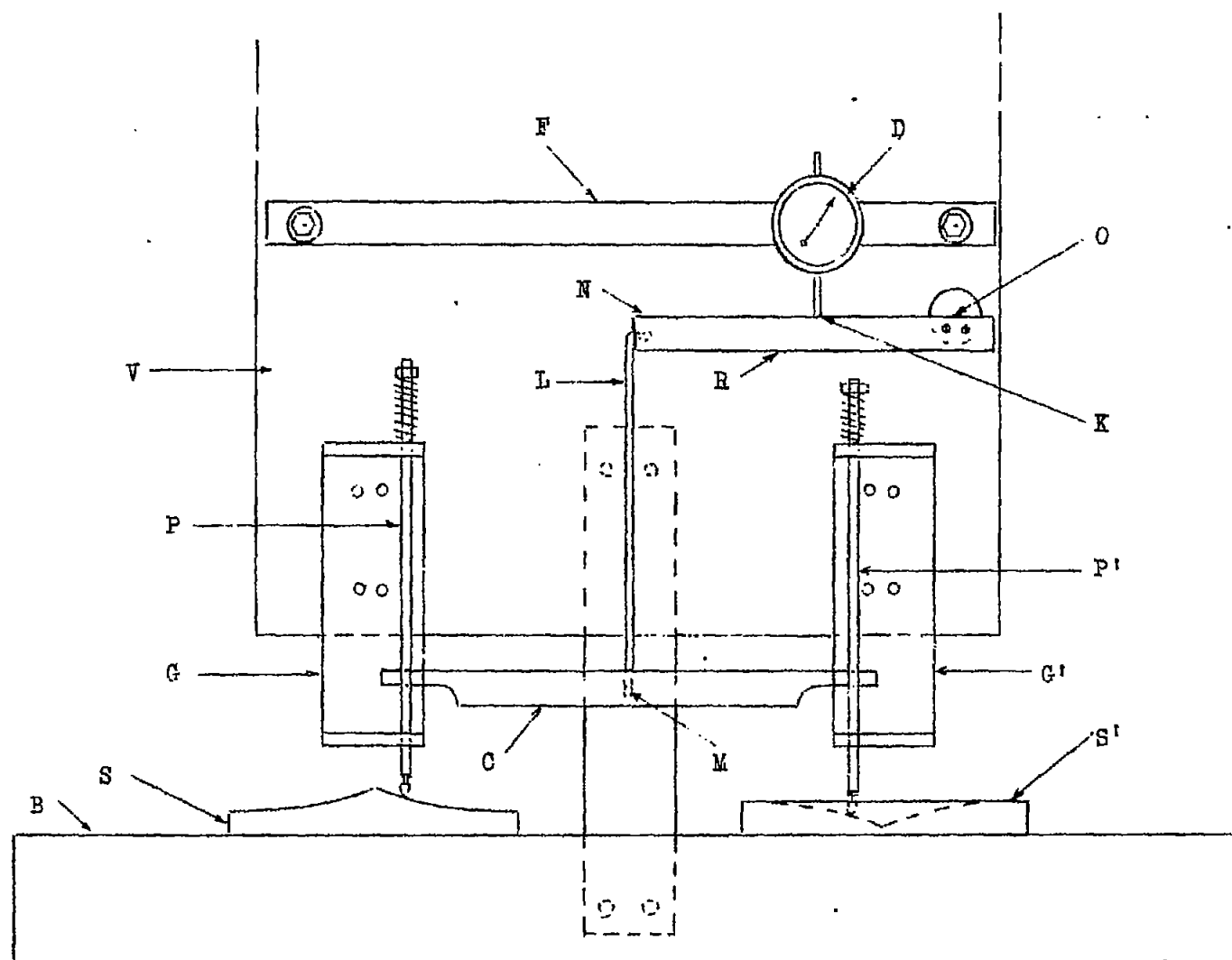


Figure 5.- Schematic drawing of one set of moving parts of the analyzer.

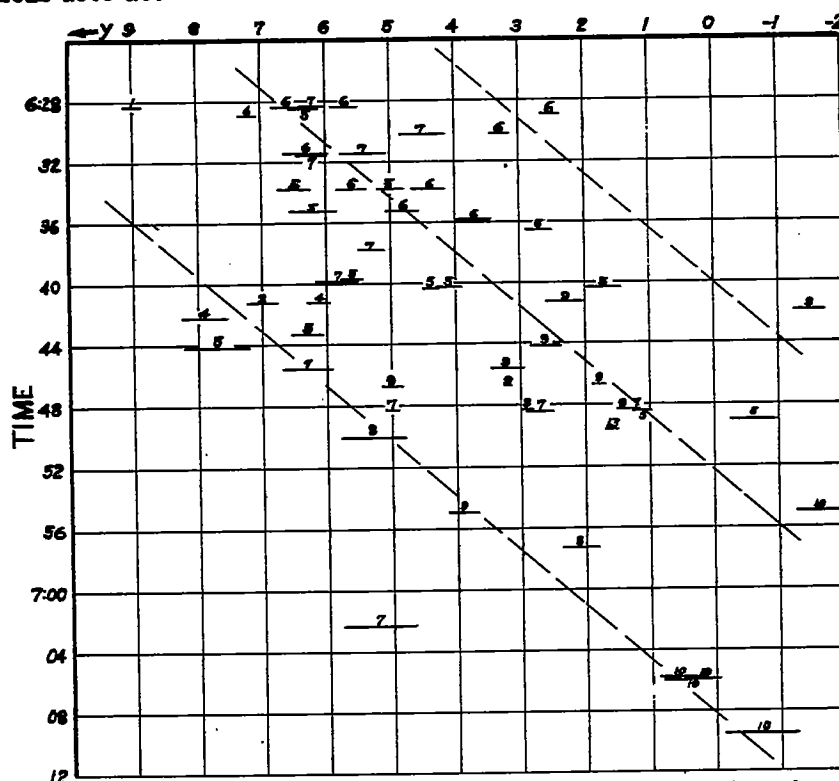
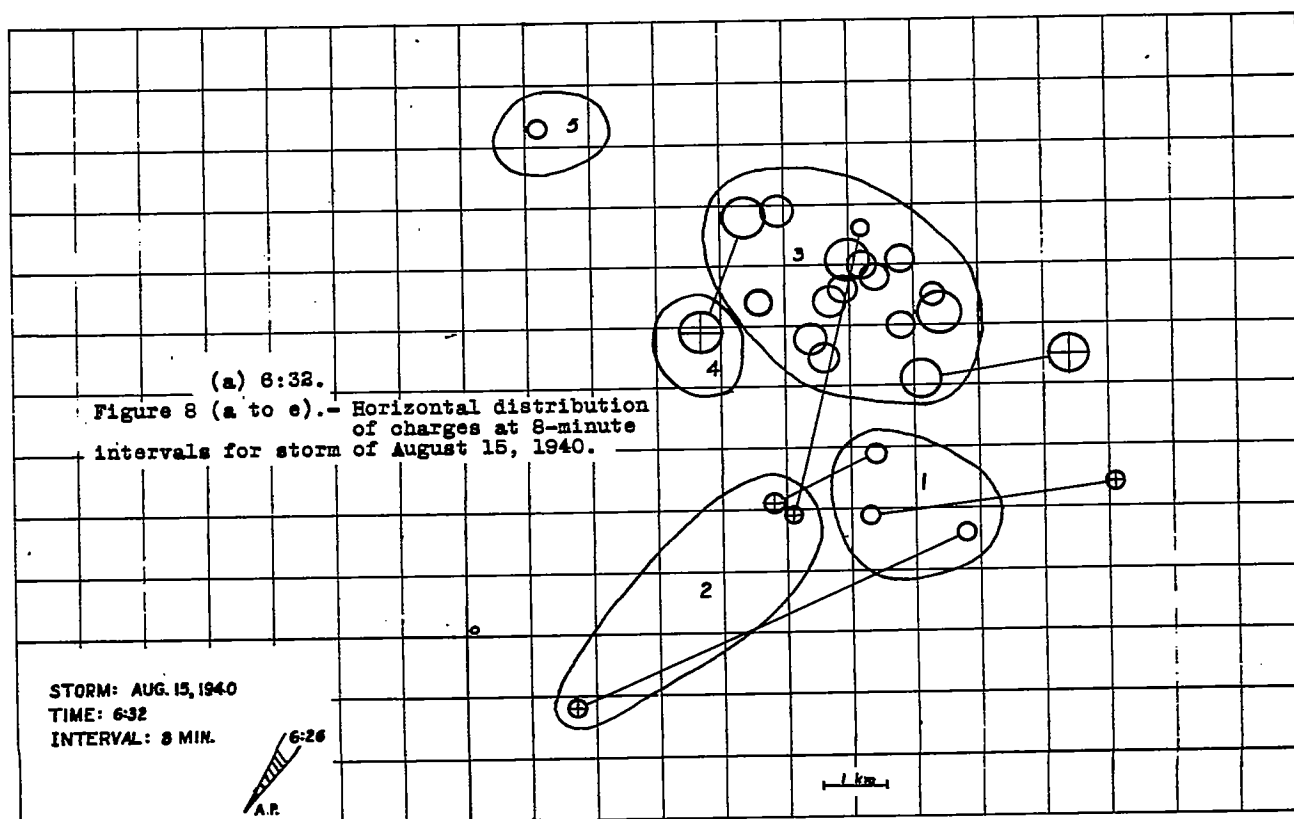
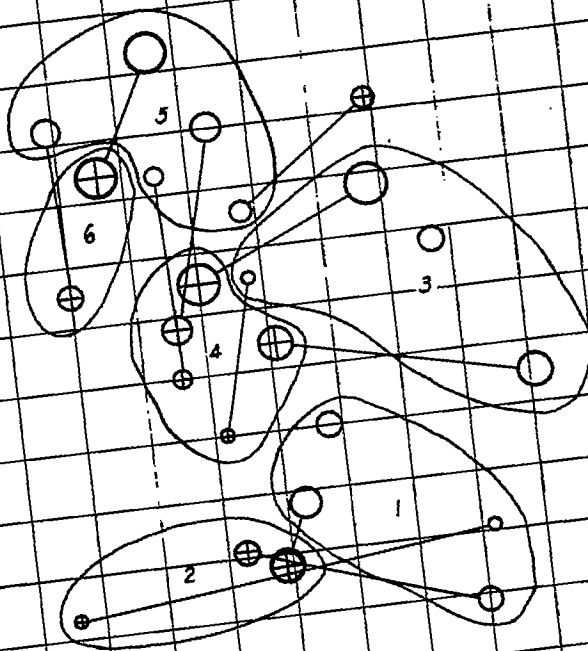


Figure 7.- Chart used to determine the approximate boundaries of negative charges, storm of August 15, showing the variation of y coordinate with time. Numbers represent x coordinates.



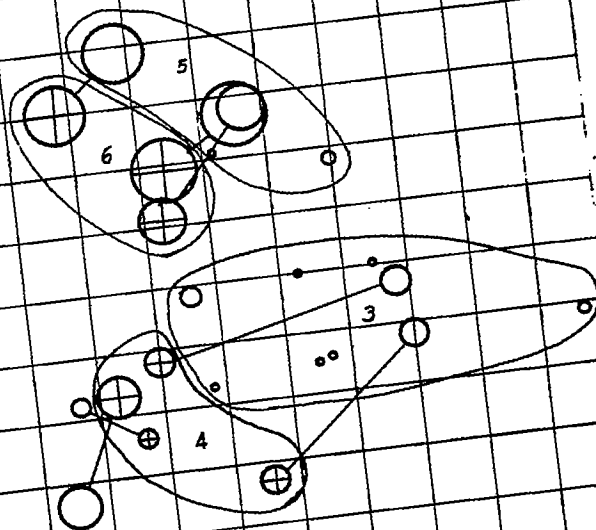
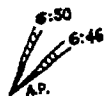
(b) 6:40.  
Figure 8.- Continued.

STORM: AUG. 15, 1940  
TIME: 6:40  
INTERVAL: 8 MIN.



(c) 6:48.  
Figure 8.- Continued.

STORM: AUG. 15, 1940  
TIME: 6:48  
INTERVAL: 8 MIN.



(d) 6:56.  
Figure 8.- Continued.

STORM: AUG. 13, 1940  
TIME: 6:56  
INTERVAL: 6 MIN.

AP

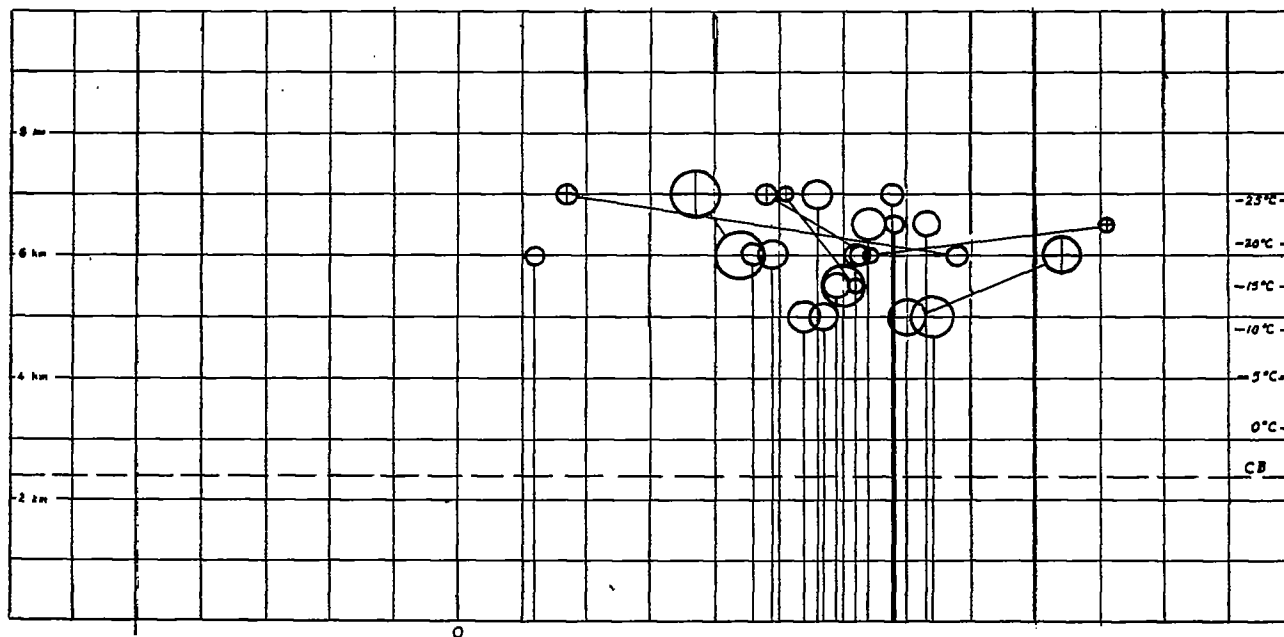
1 km

(e) 7:04.  
Figure 8.- Concluded.

STORM: AUG. 13, 1940  
TIME: 7:04  
INTERVAL: 6 MIN.

7:02  
AP 7:02

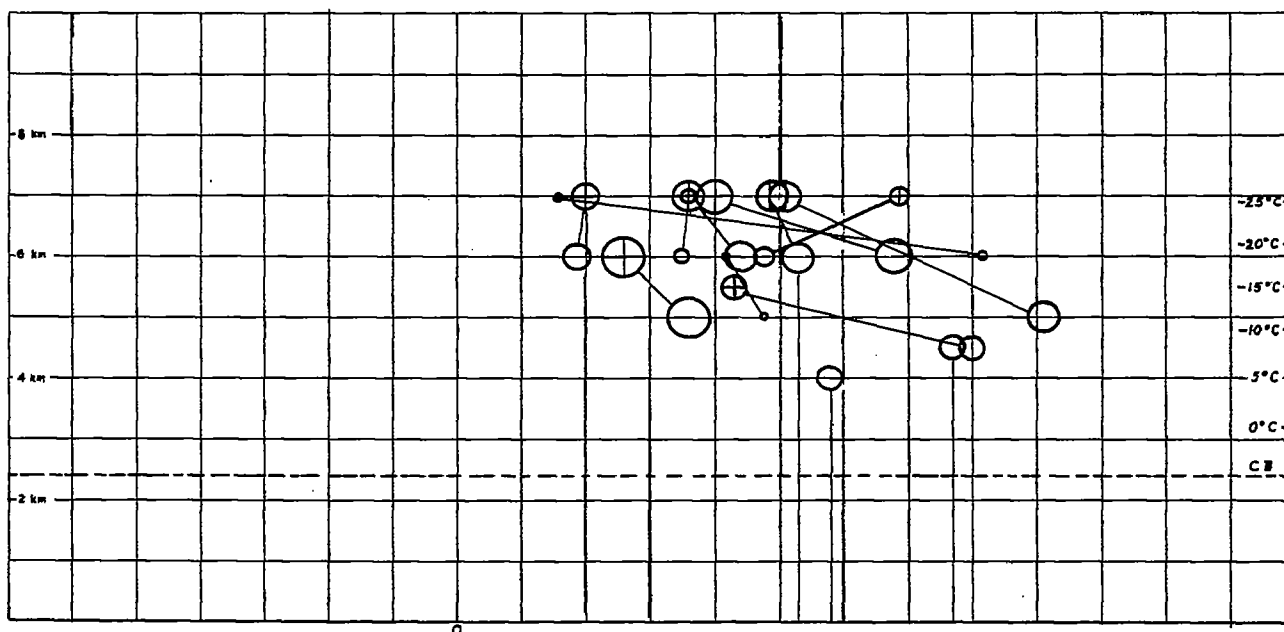
1 km



STORM: AUG. 15, 1940  
 TIME: 6:32  
 INTERVAL: 6 MIN.

(a) 6:32.

Figure 9 (a to e).— Vertical distribution of charges at 8-minute intervals for storm of August 15, 1940.

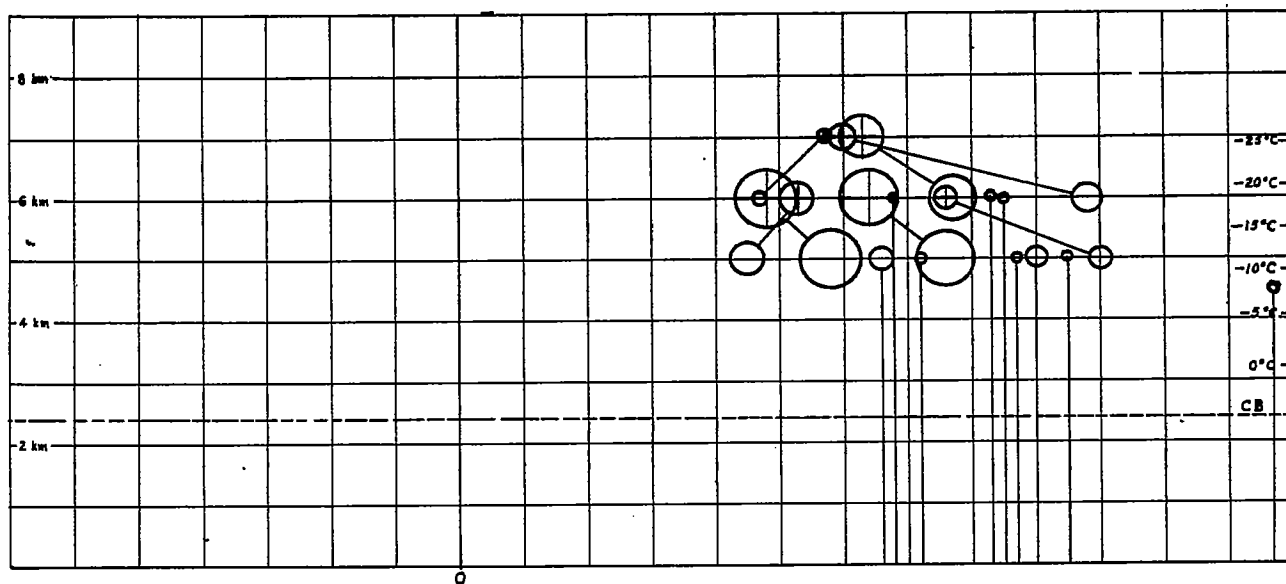


STORM: AUG. 15, 1940  
 TIME: 6:40  
 INTERVAL: 6 MIN.

(b) 6:40.

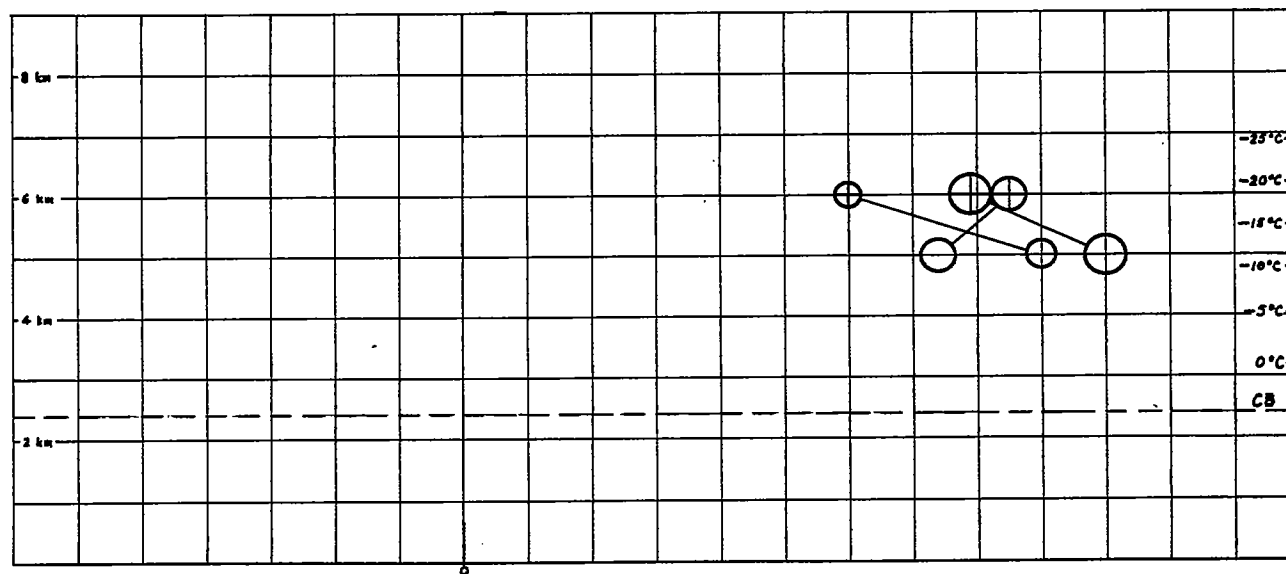
Figure 9.— Continued.





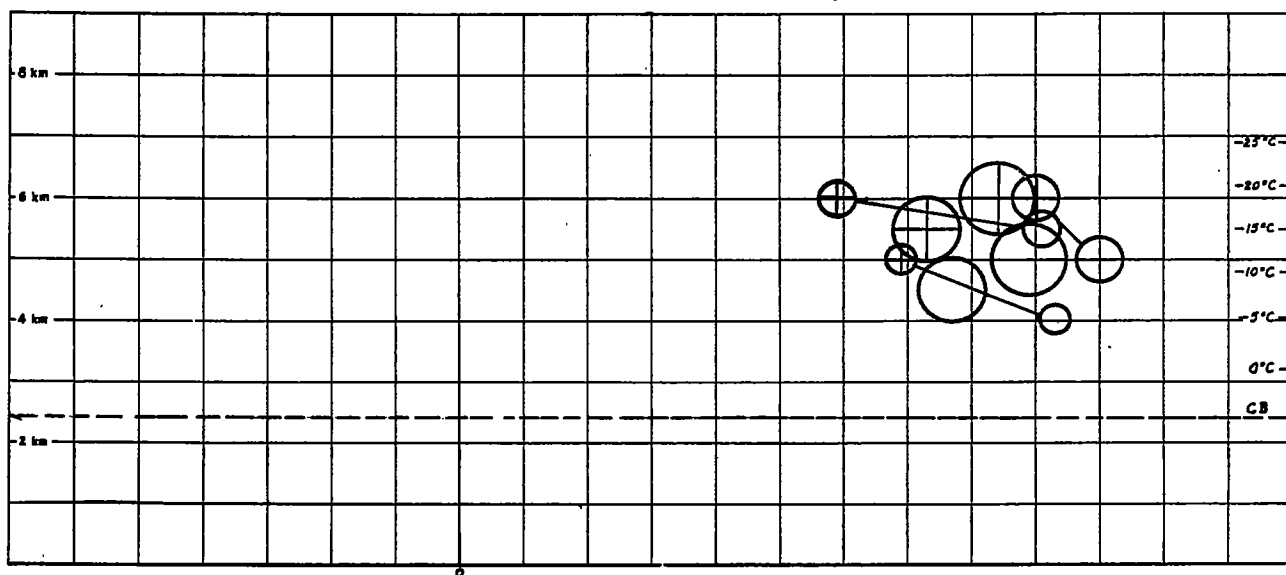
STORM: AUG. 15, 1940  
TIME: 6:48  
INTERVAL: 8 MIN.

(c) 6:48.  
Figure 9.- Continued.



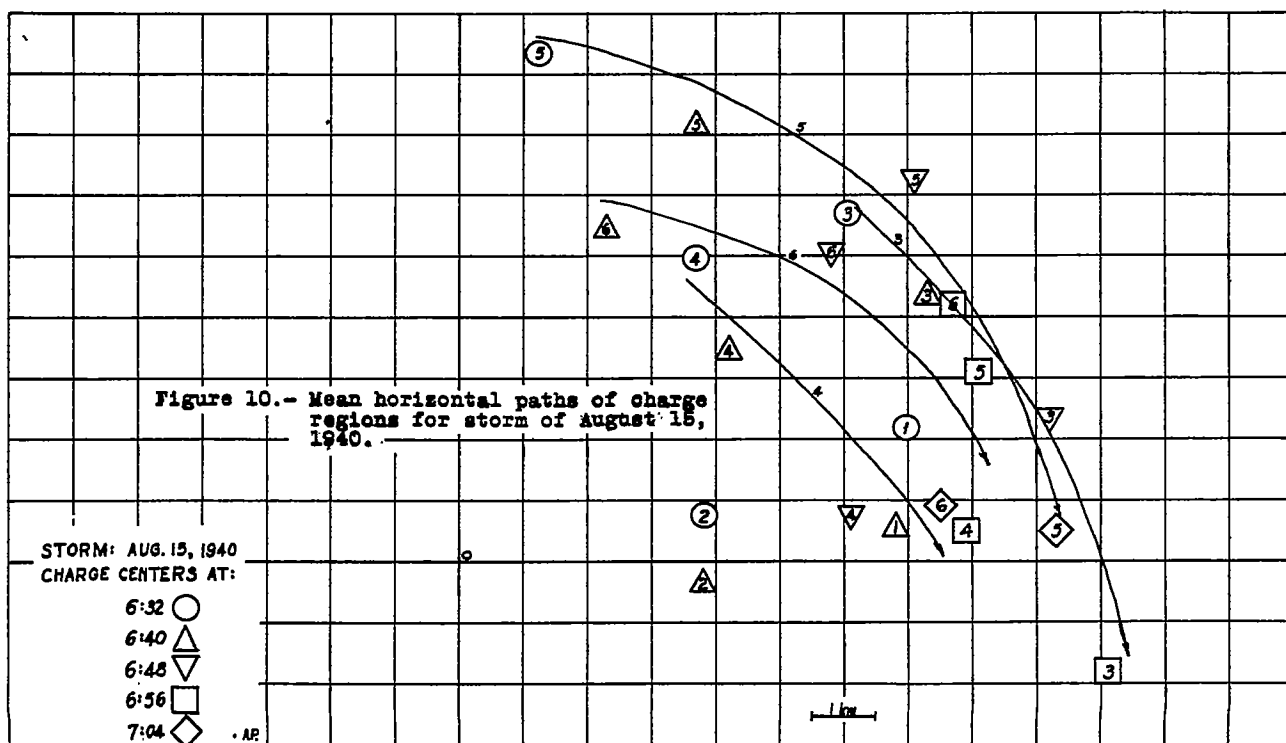
STORM: AUG. 15, 1940  
TIME: 6:56  
INTERVAL: 8 MIN.

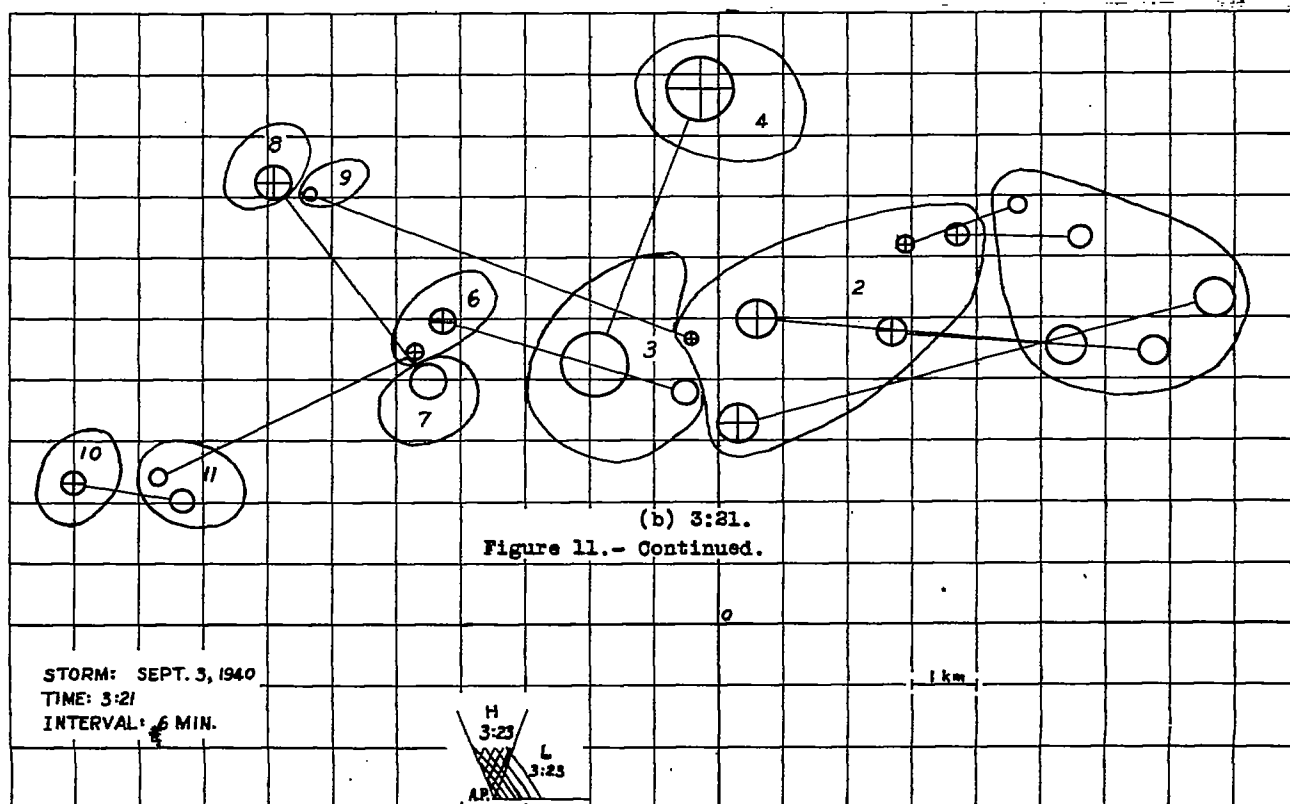
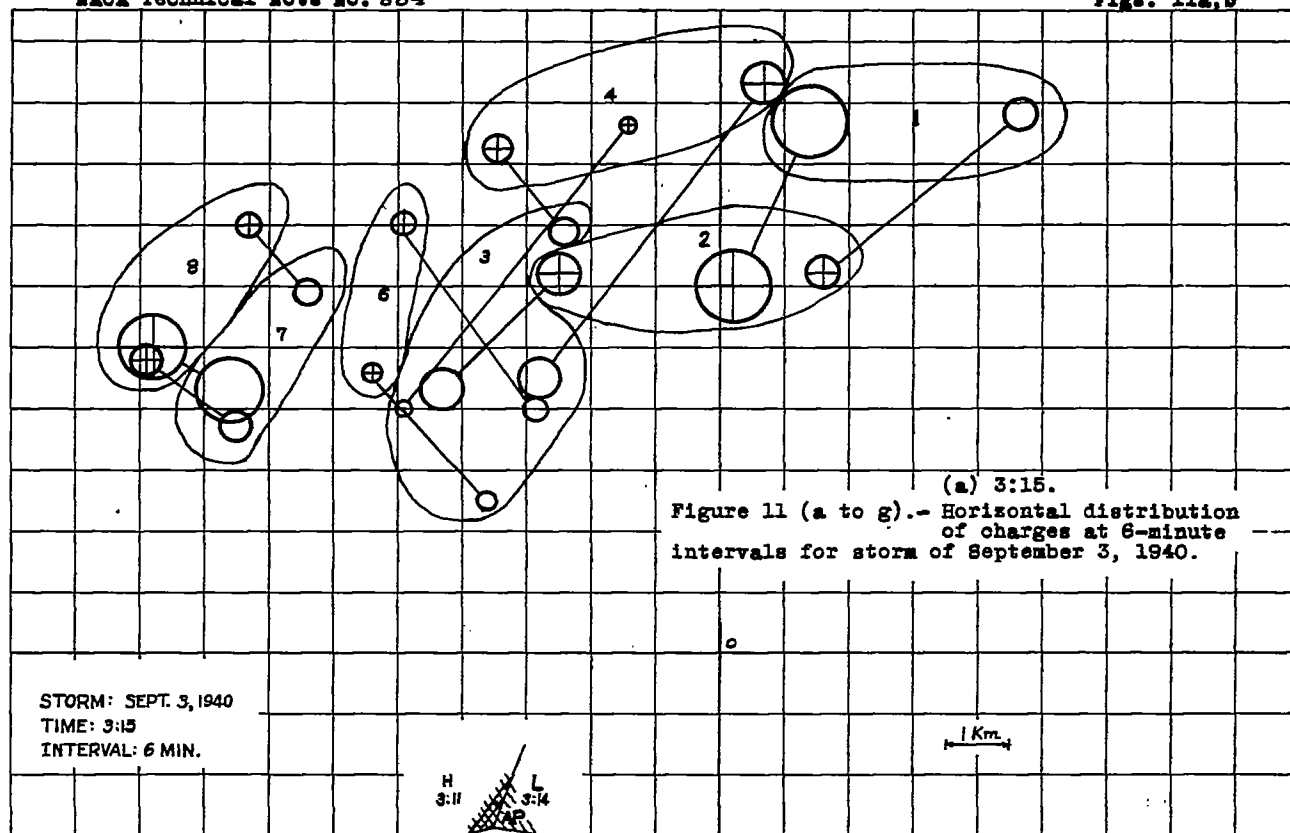
(d) 6:56.  
Figure 9.- Continued.

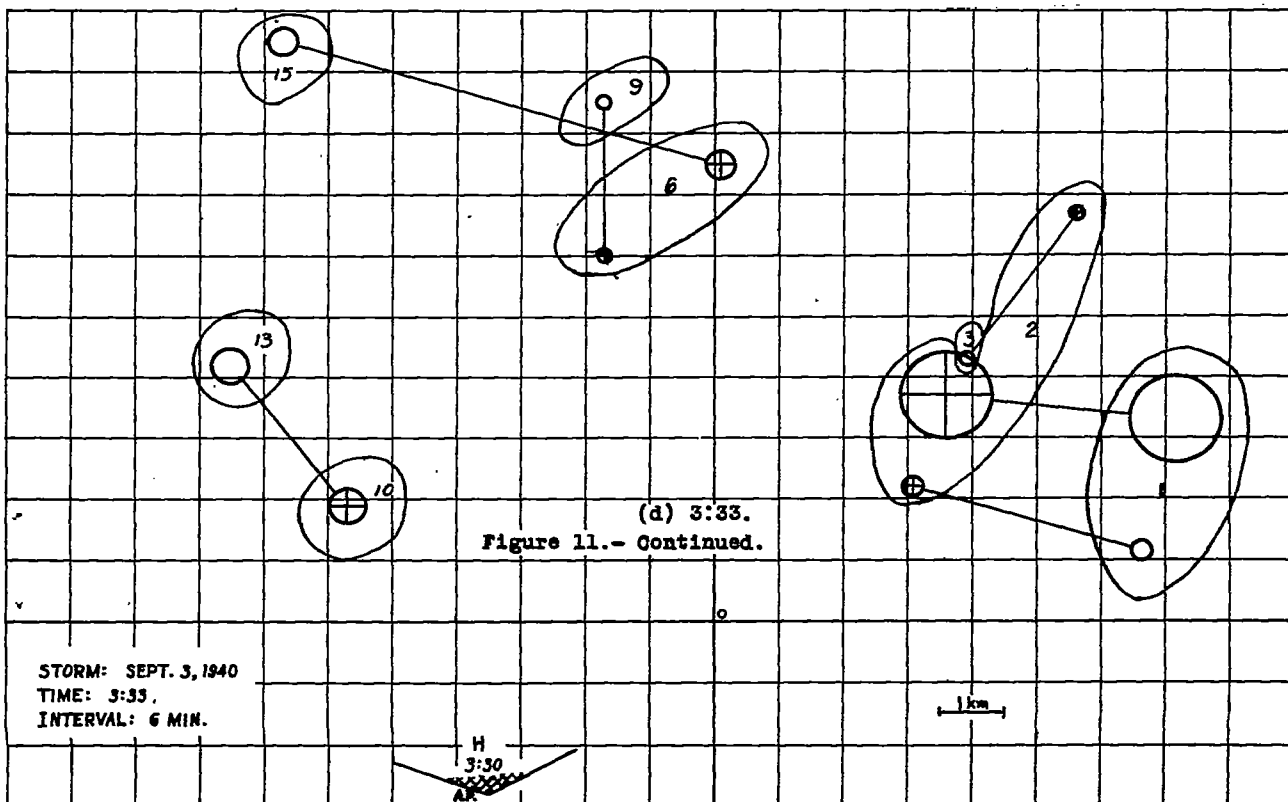
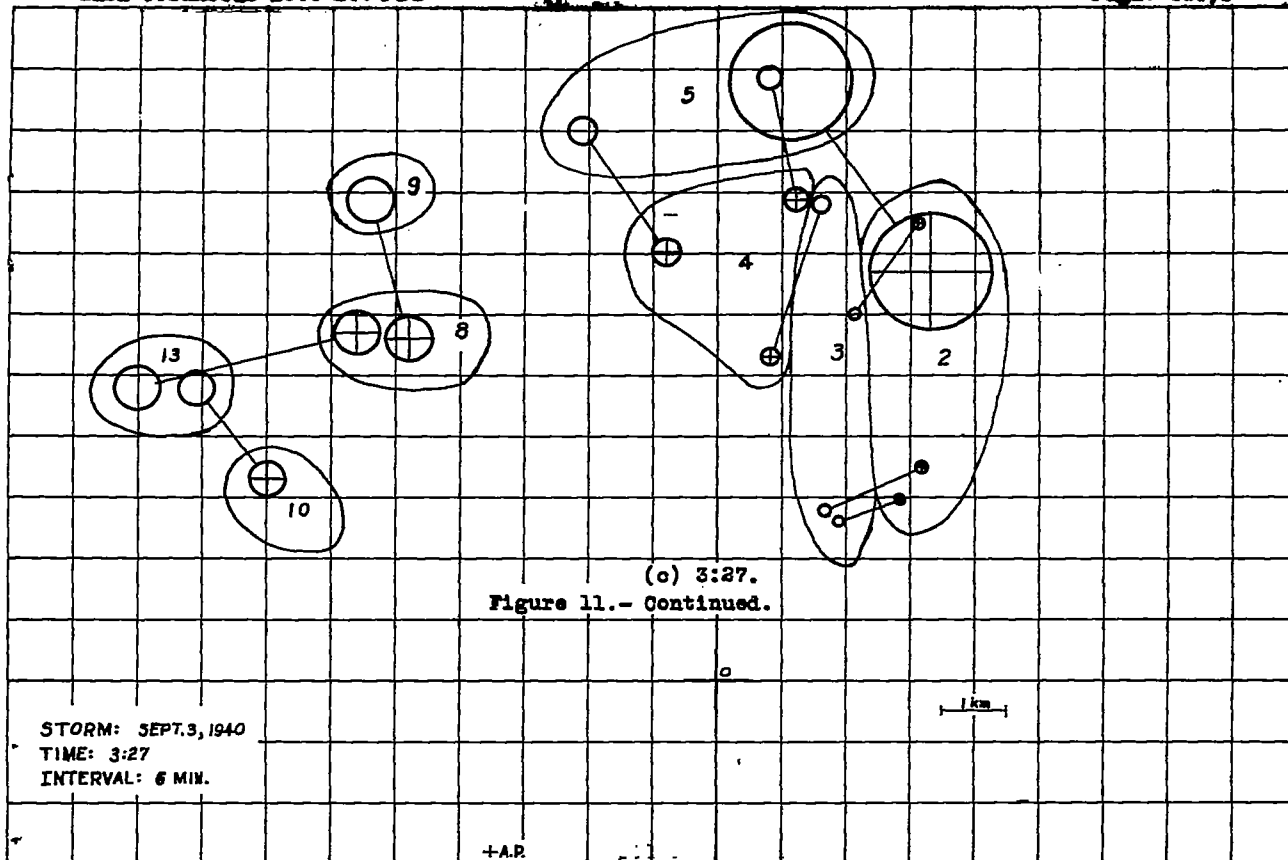


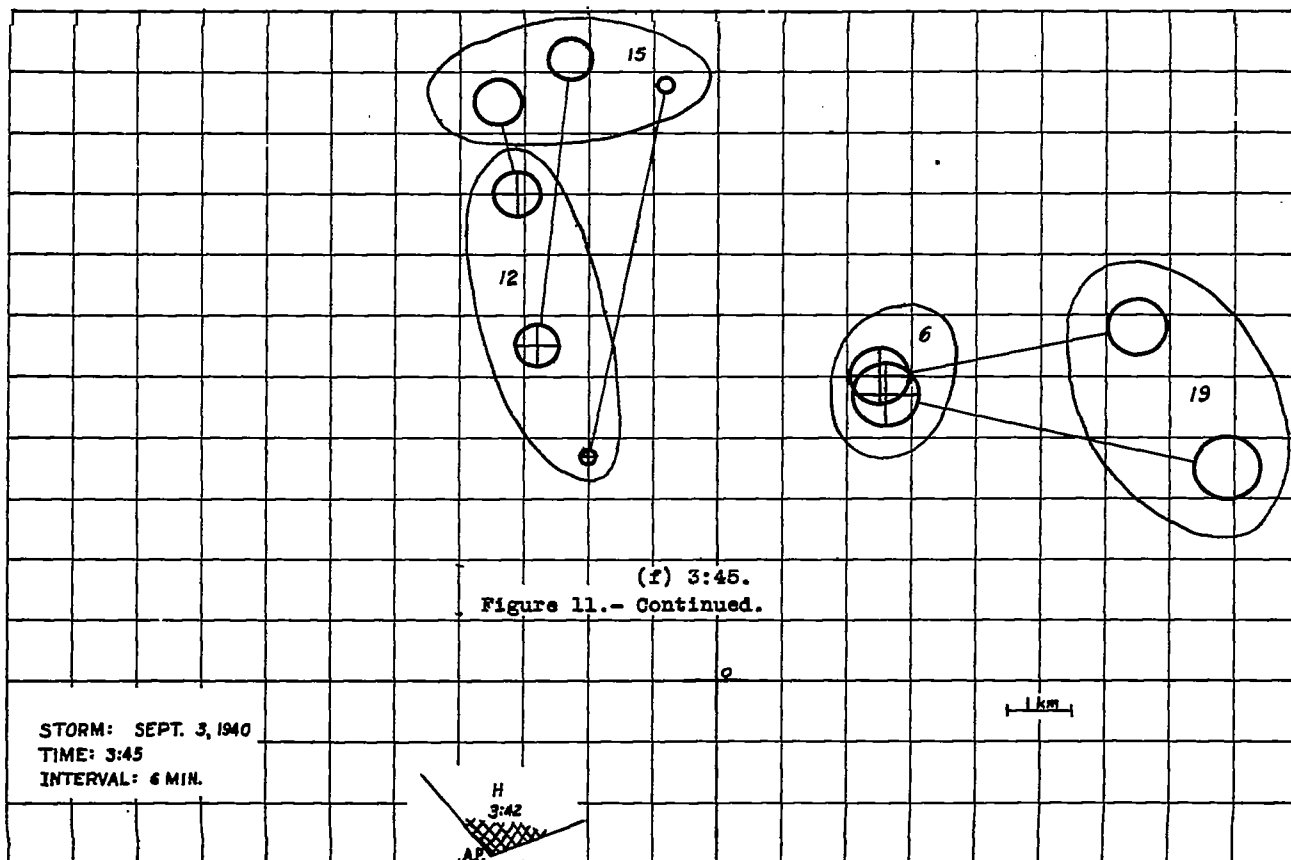
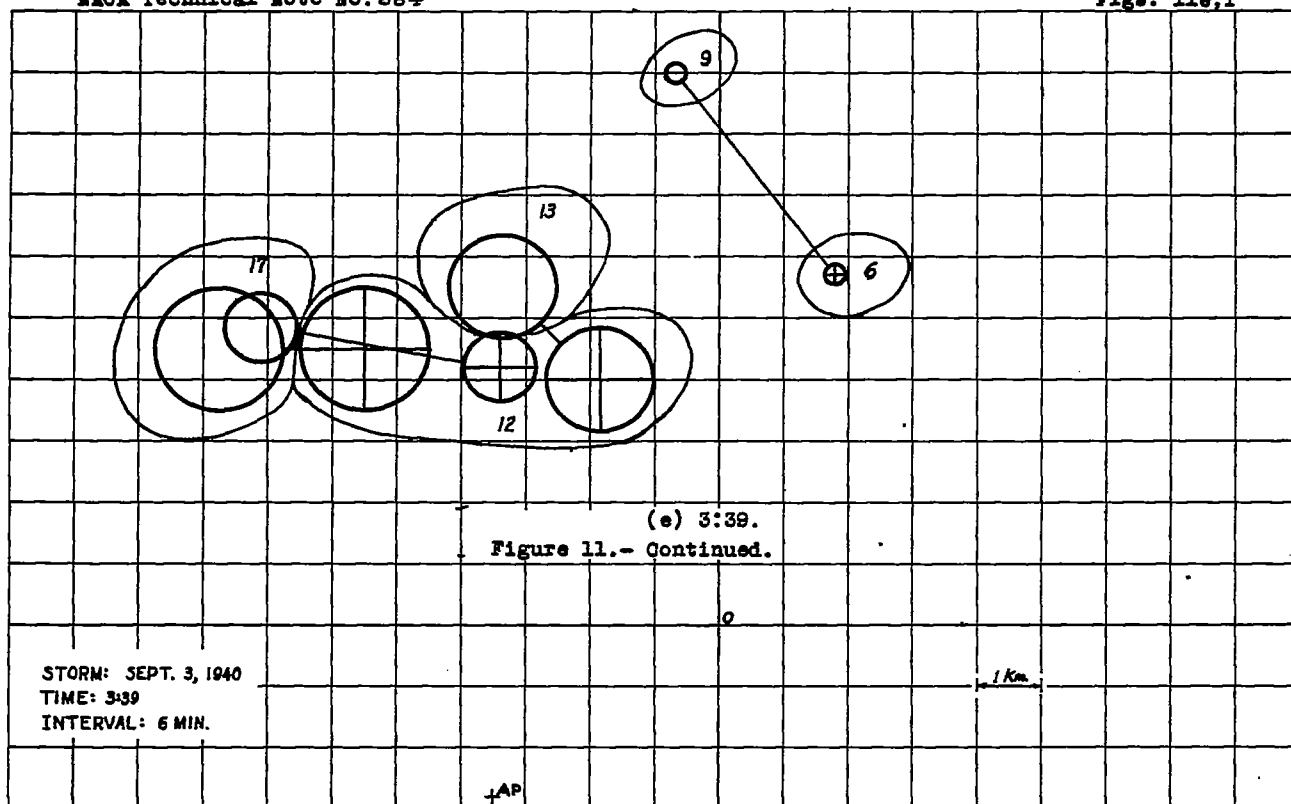
STORM: AUG. 15, 1940  
TIME: 7:04  
INTERVAL: 8 MIN.

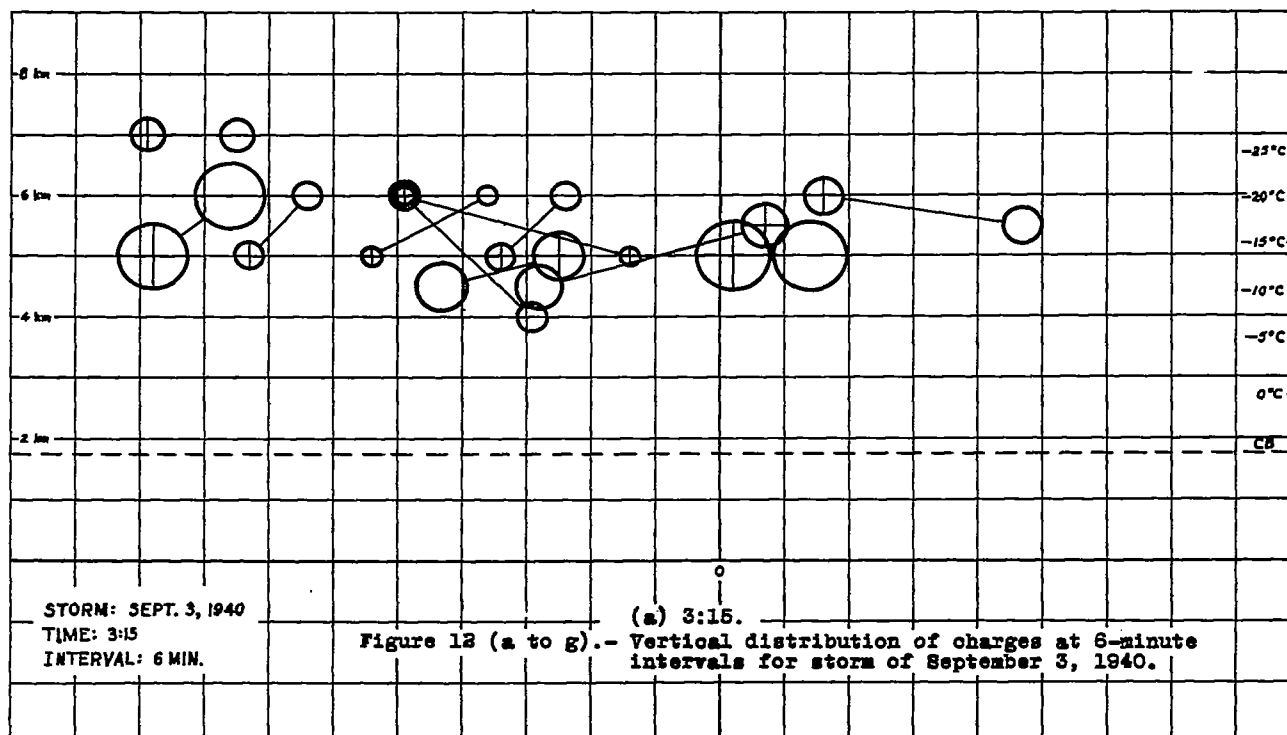
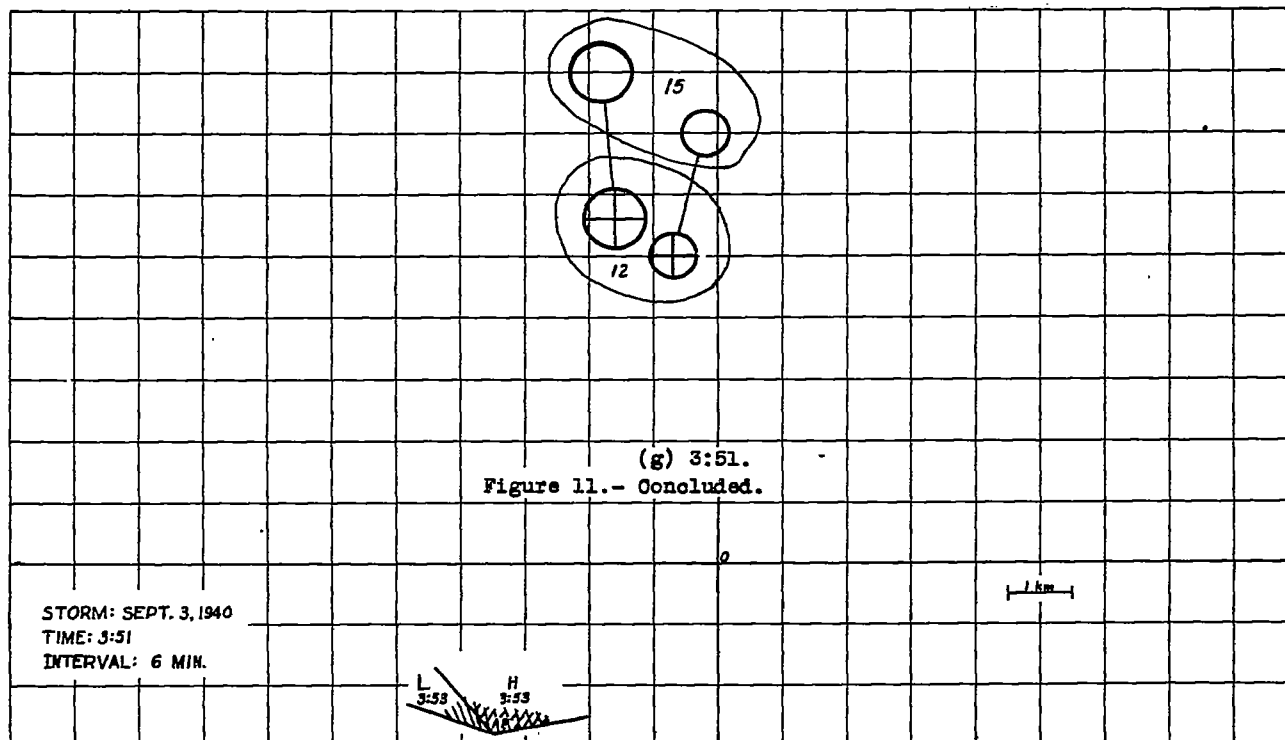
(e) 7:04.  
Figure 9.- Concluded.

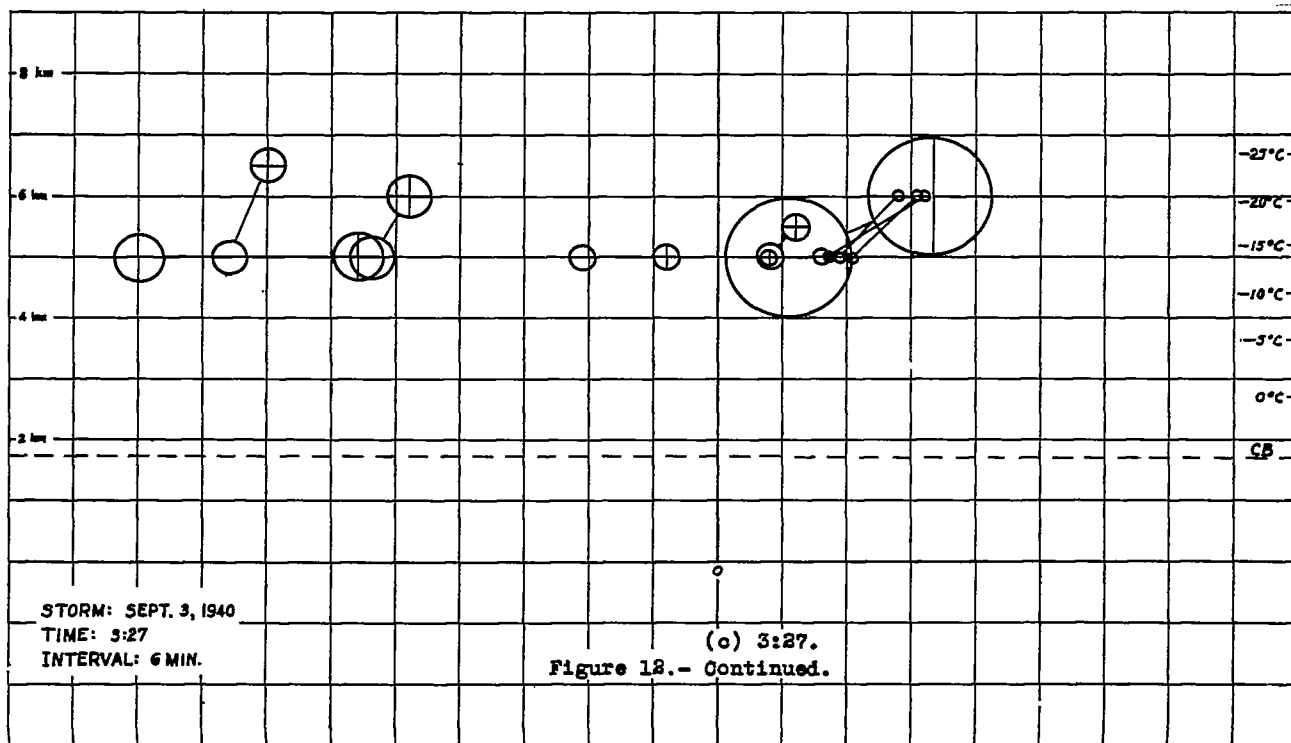
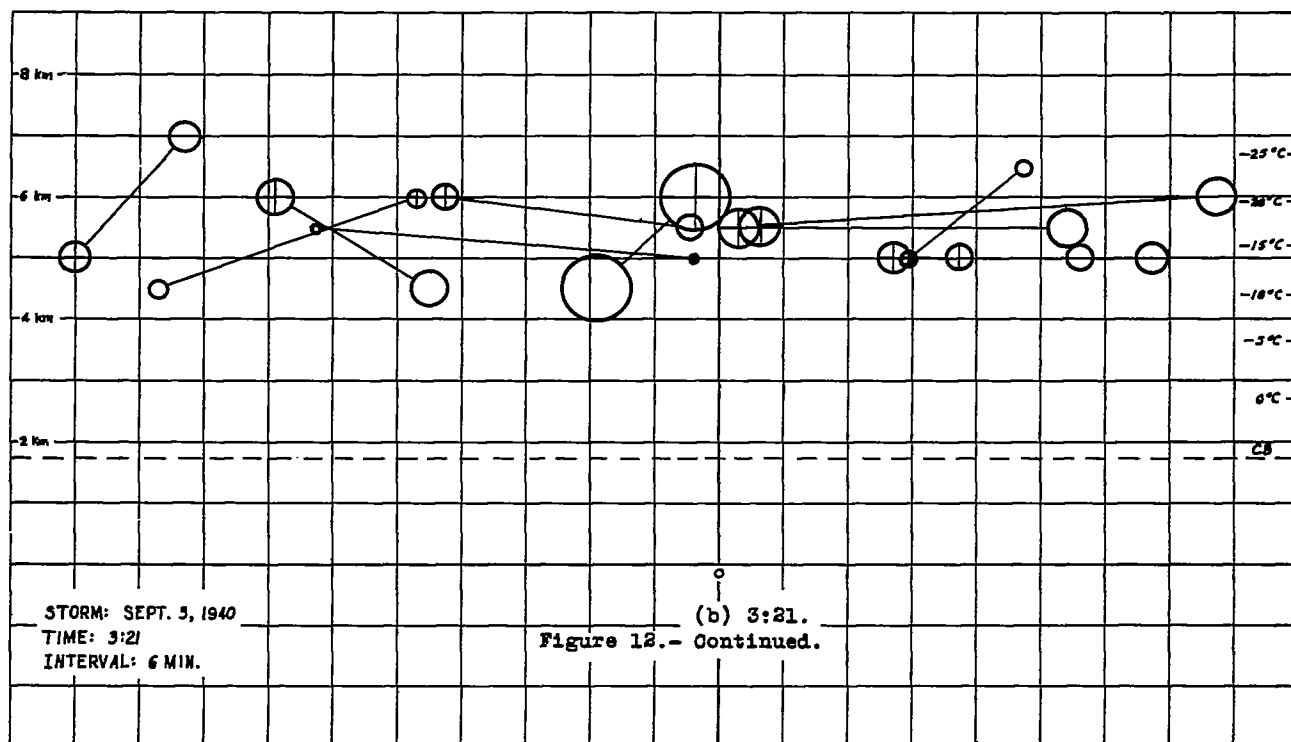


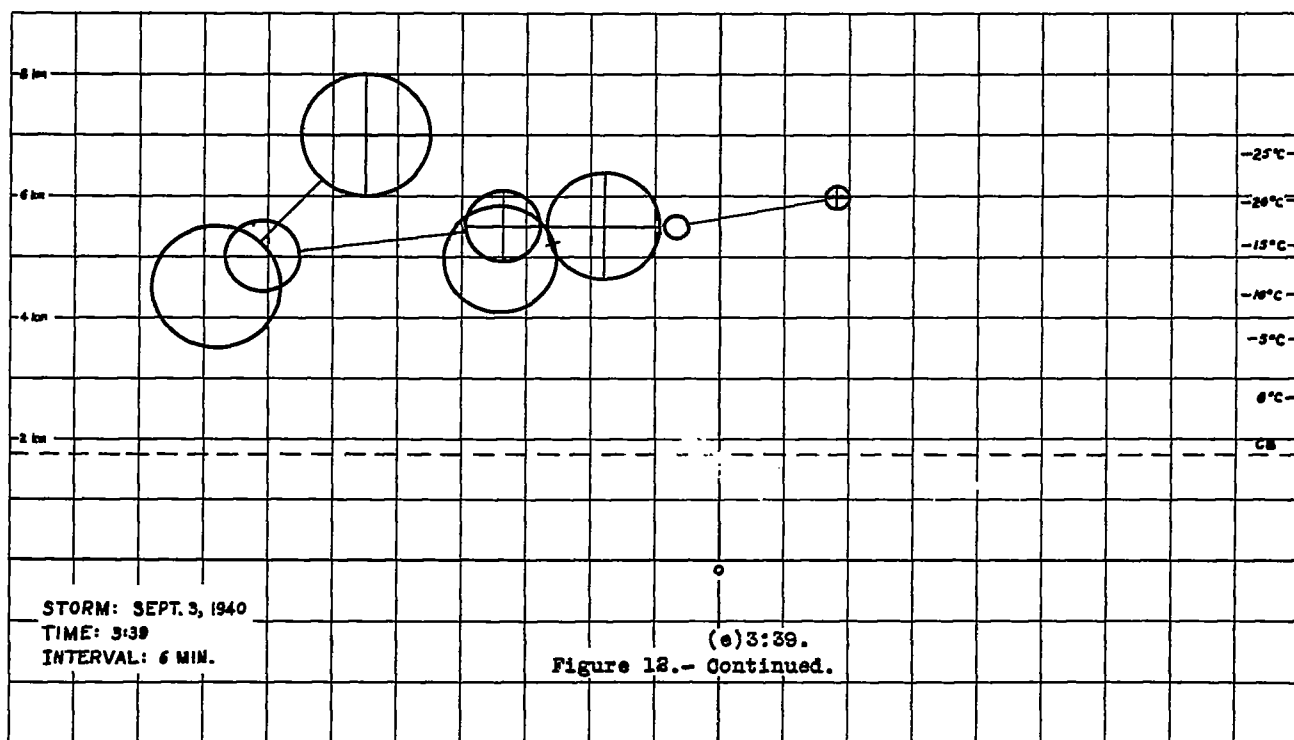
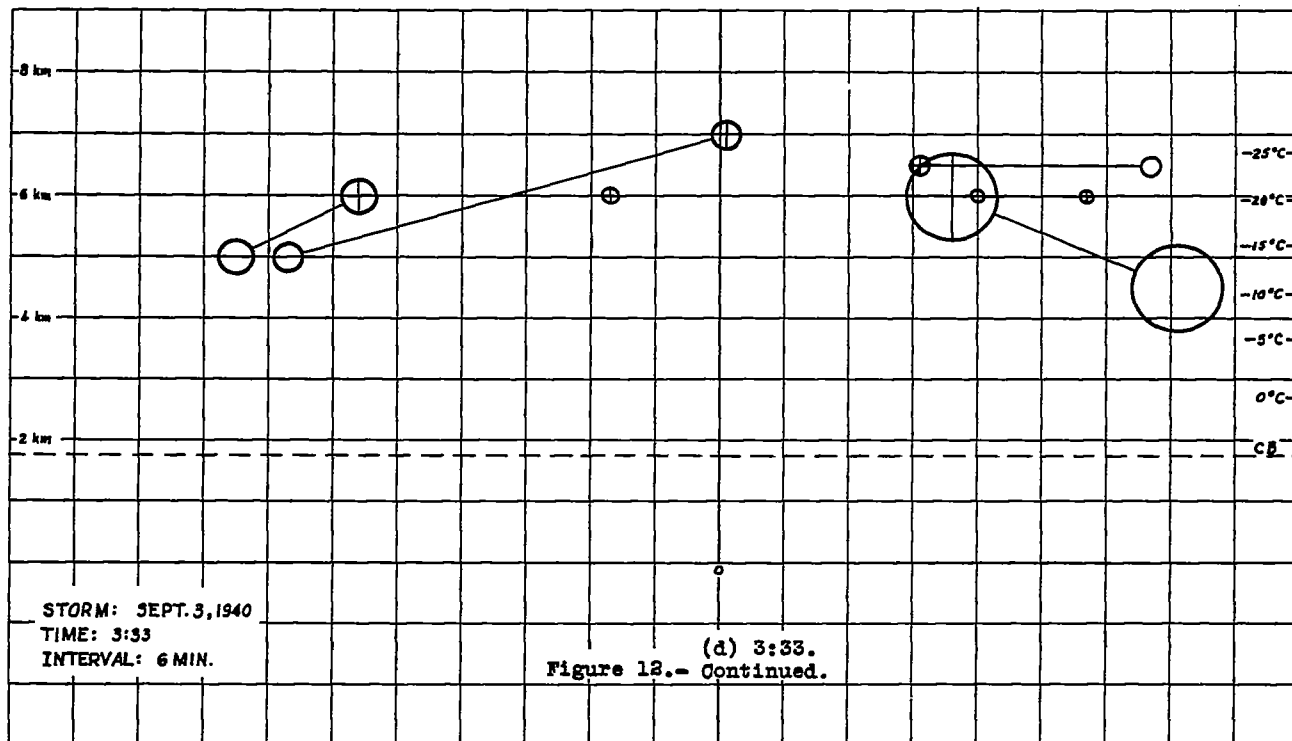




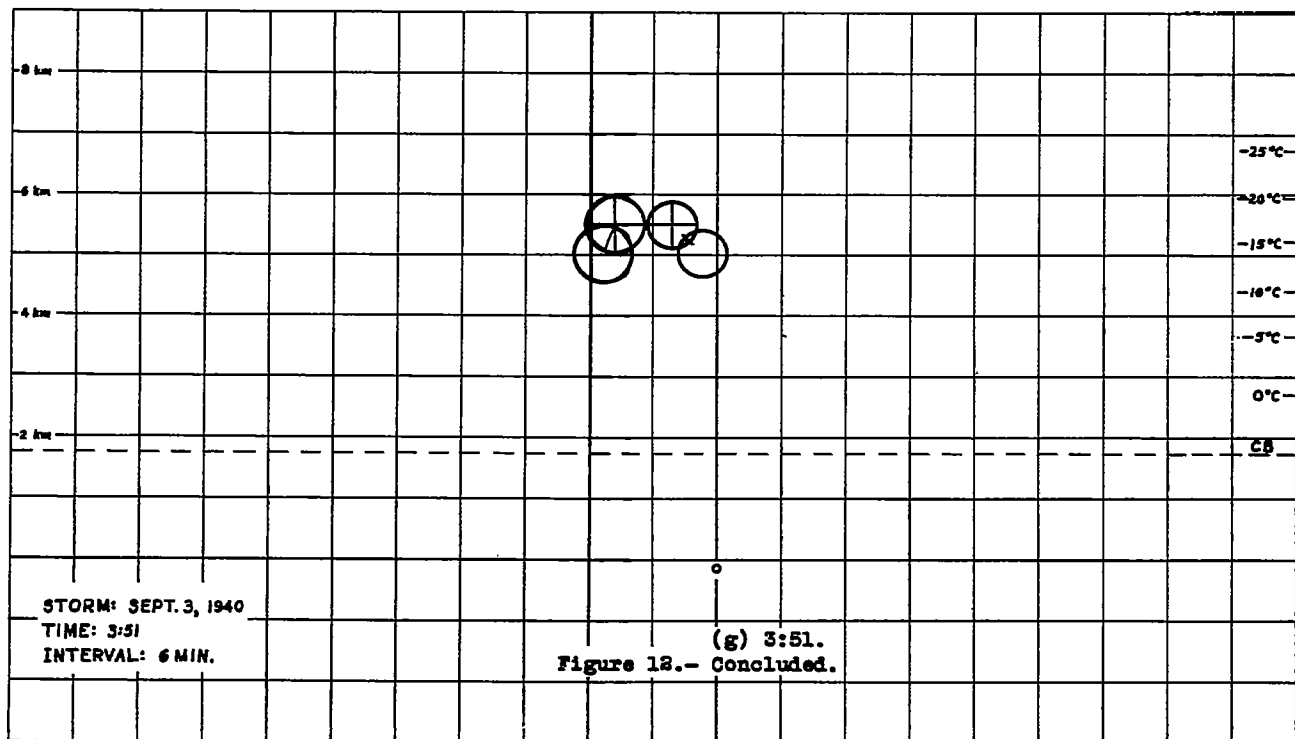
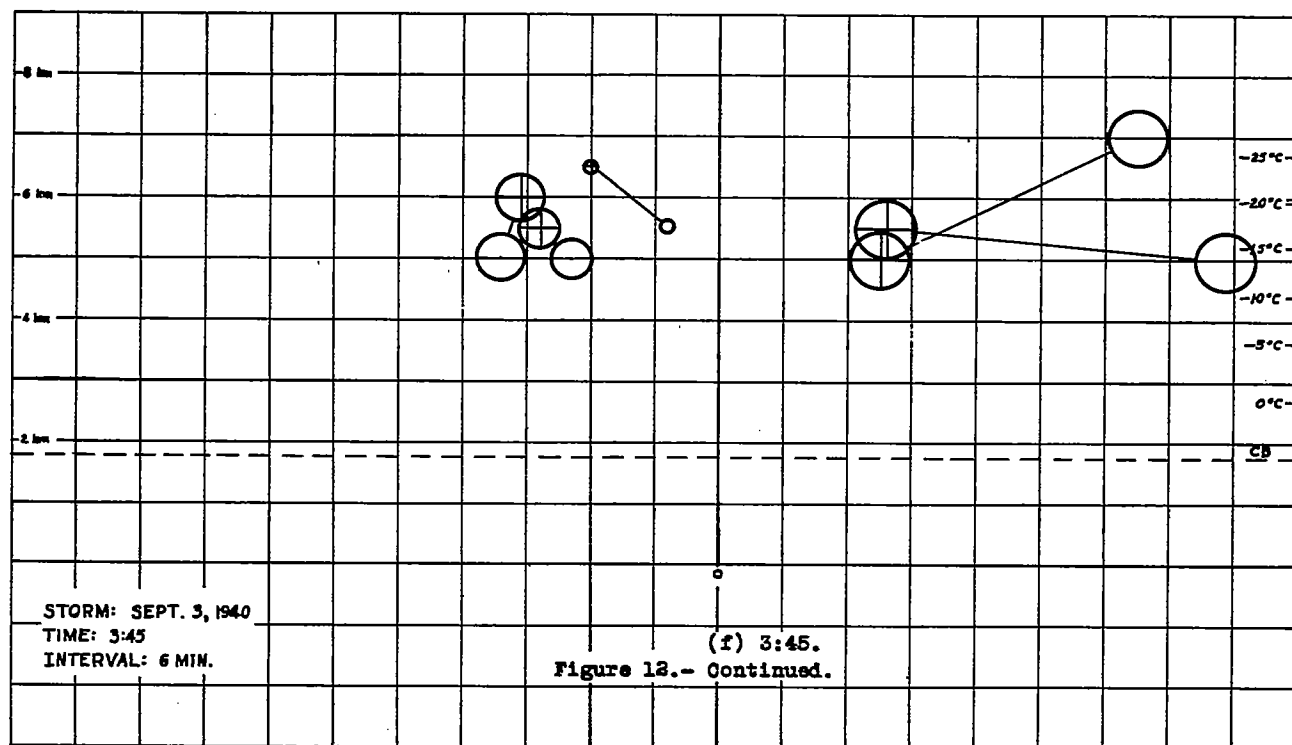


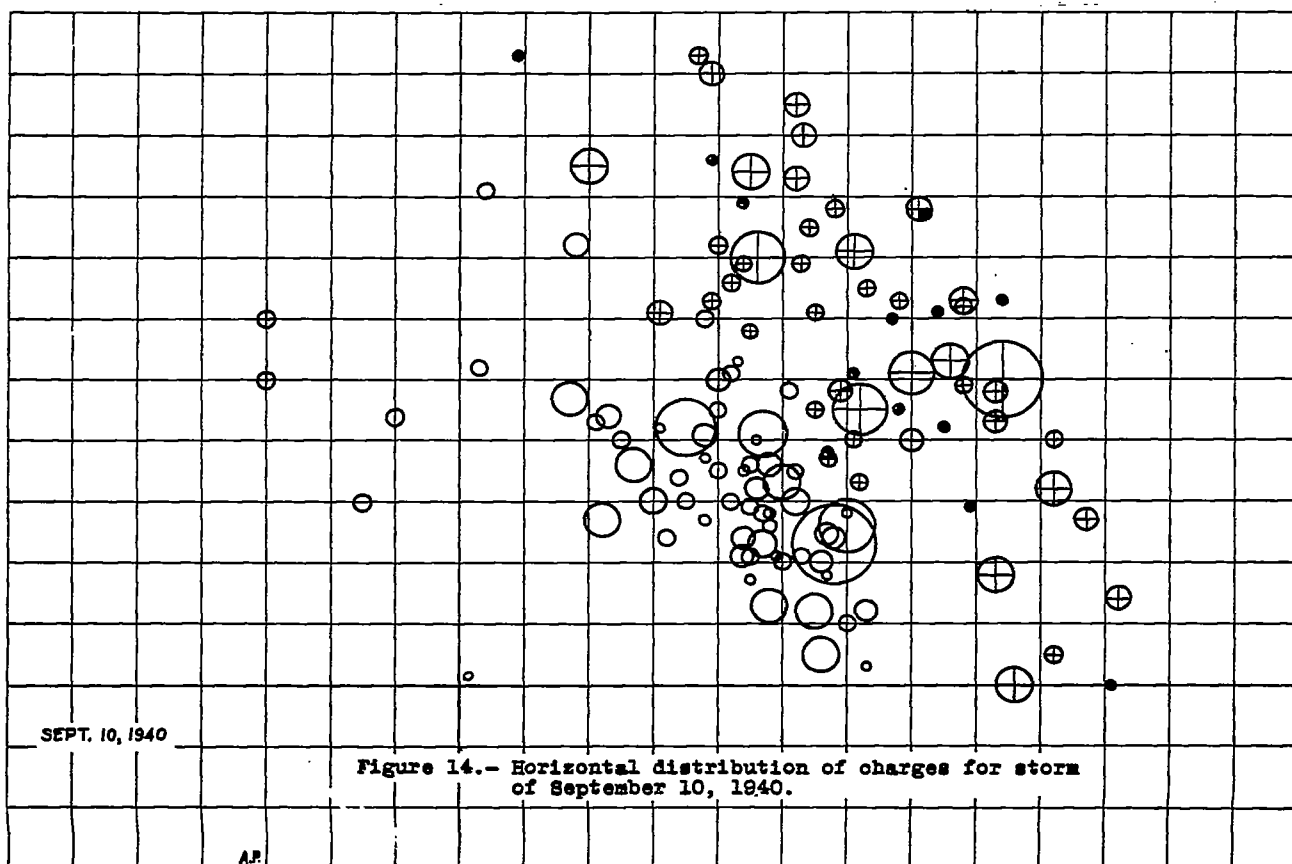
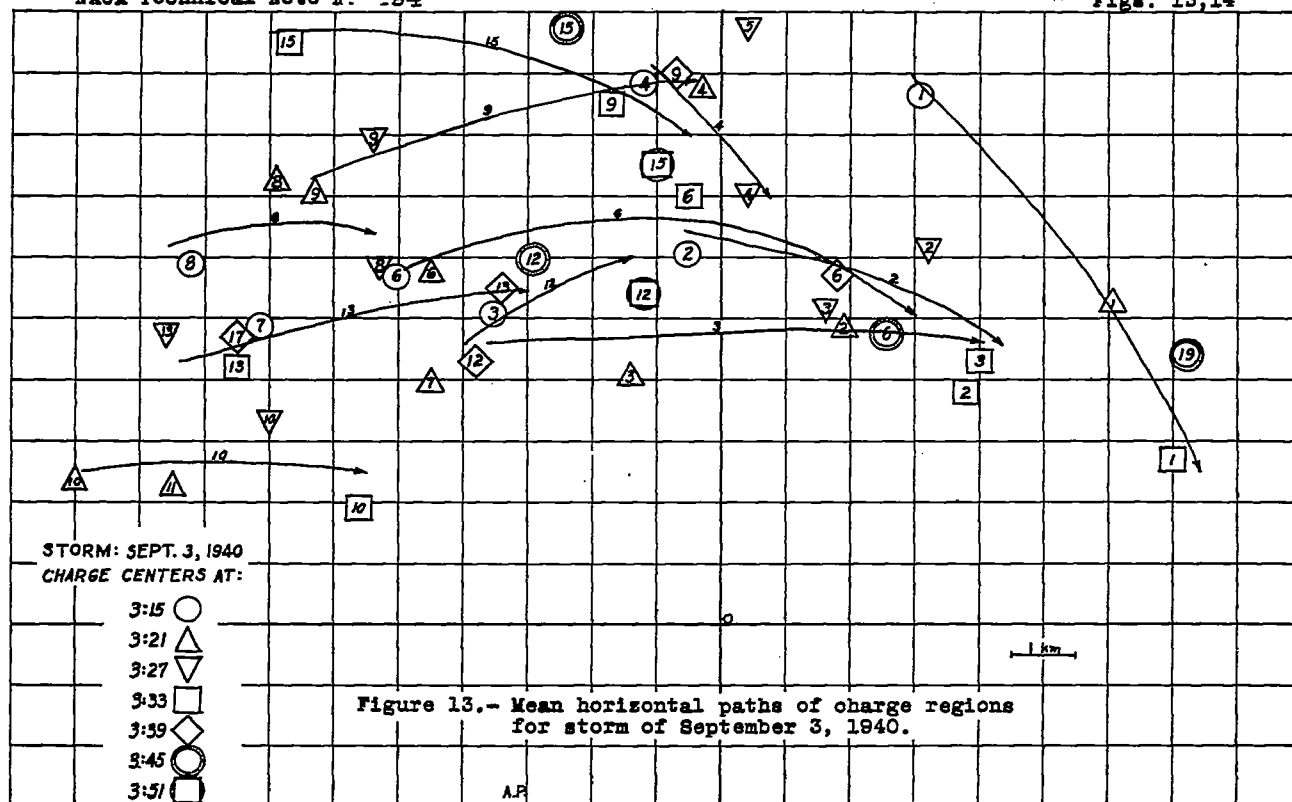


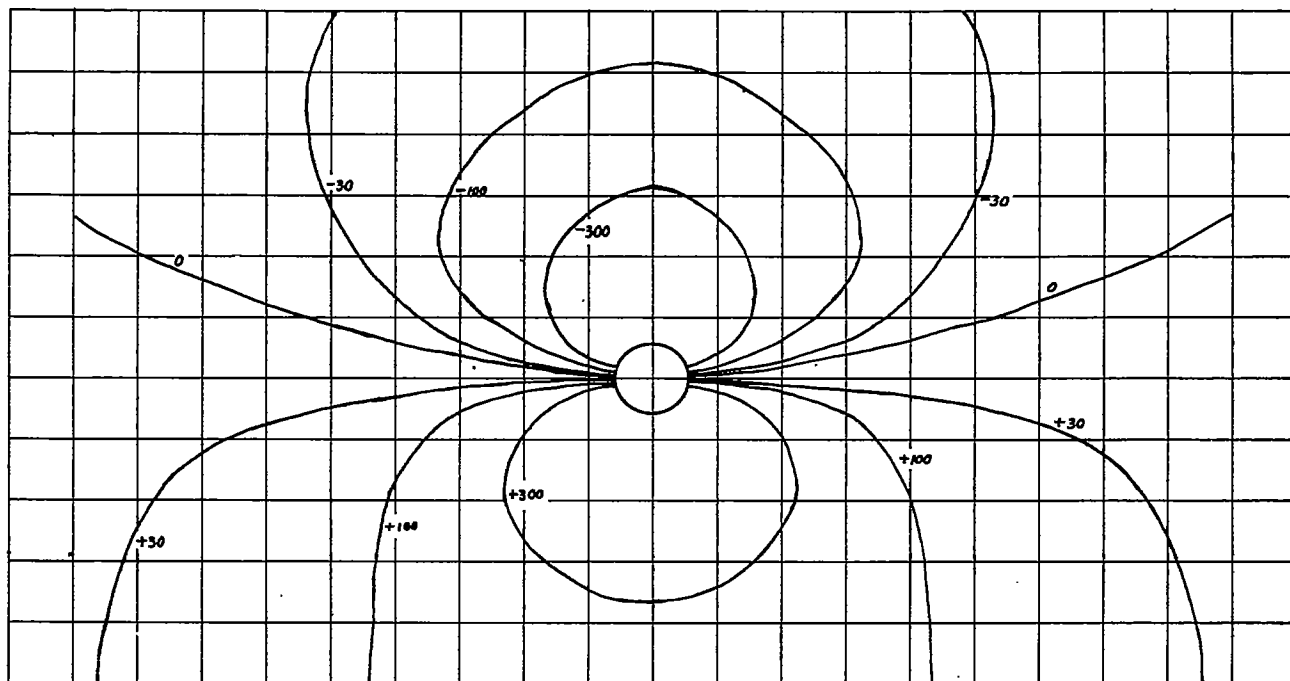








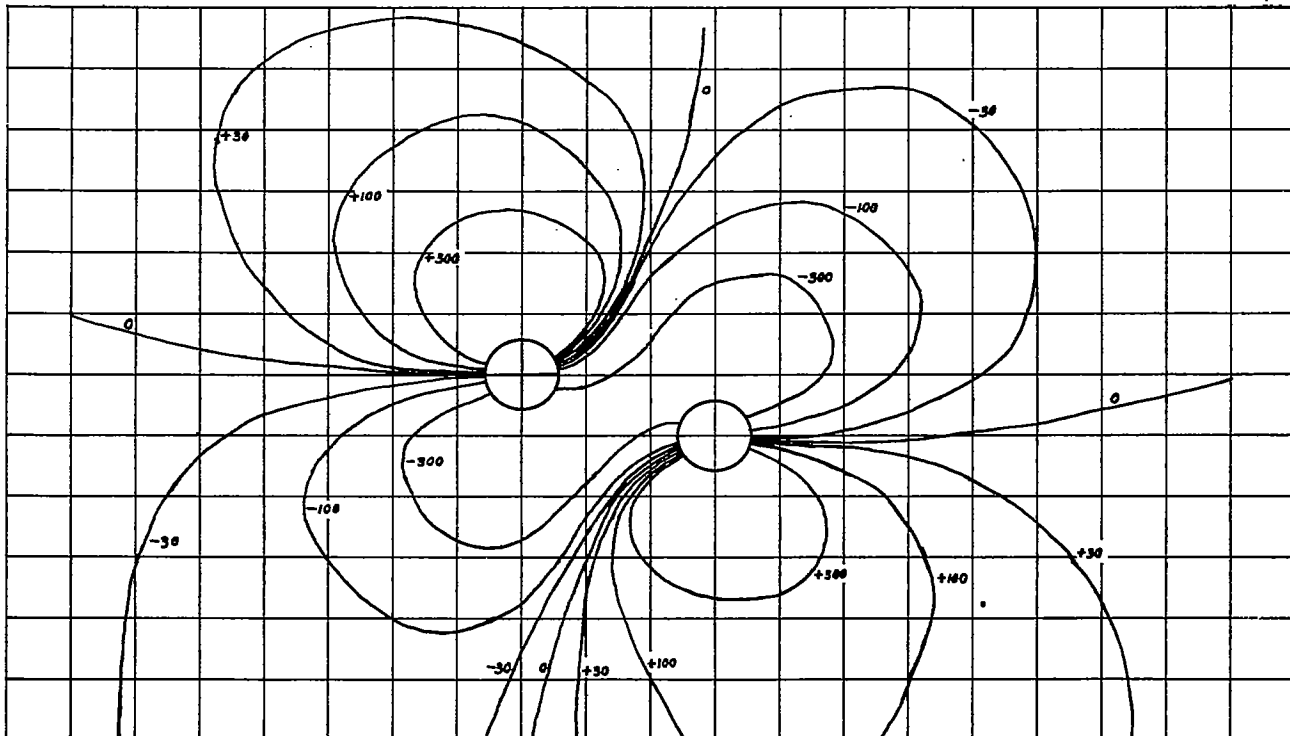




DISTRIBUTION OF VERTICAL GRADIENTS

Figure 15a.- A single 33-coulomb charge at 5 kilometers above the surface.

1 km



DISTRIBUTION OF VERTICAL GRADIENTS

Figure 15b.- Two 33-coulomb charges of opposite sign at 5 and 6 kilometers above the surface, respectively.

1 km

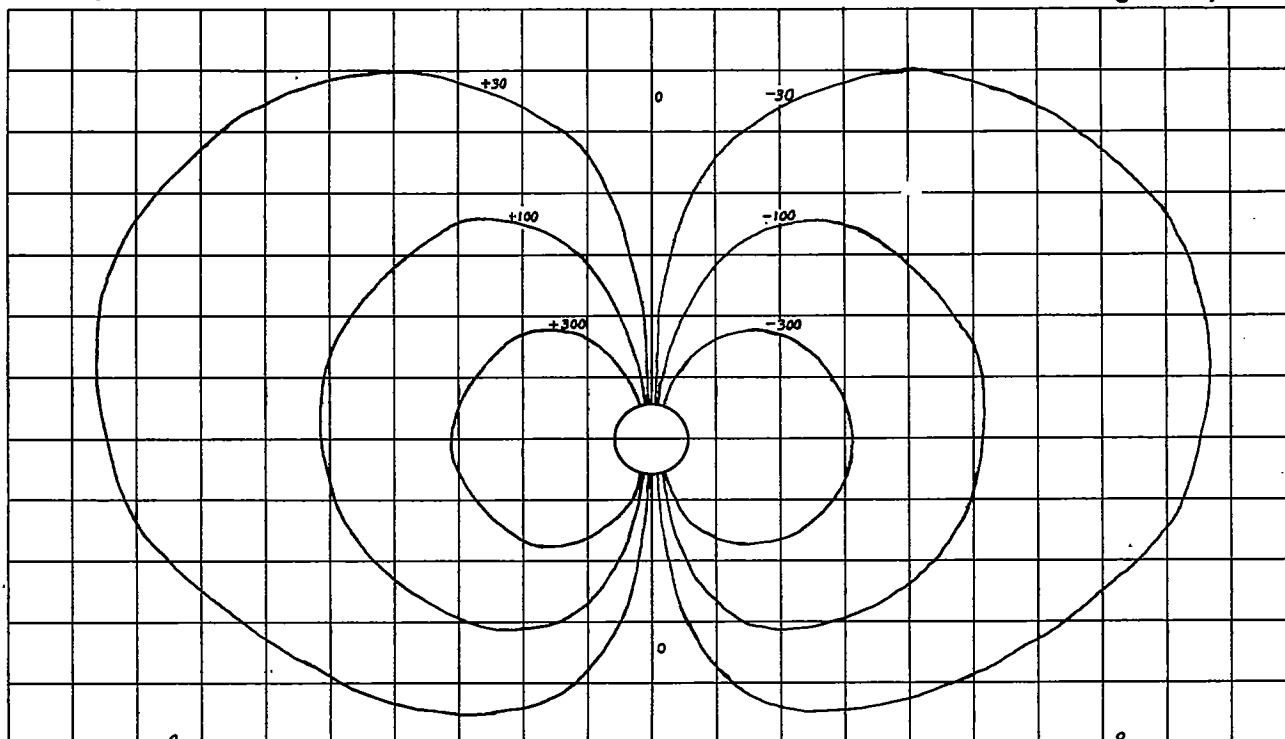


Figure 16a.- A single 33-coulomb charge at 5 kilometers above the surface.

DISTRIBUTION OF HORIZONTAL GRADIENTS

1 km

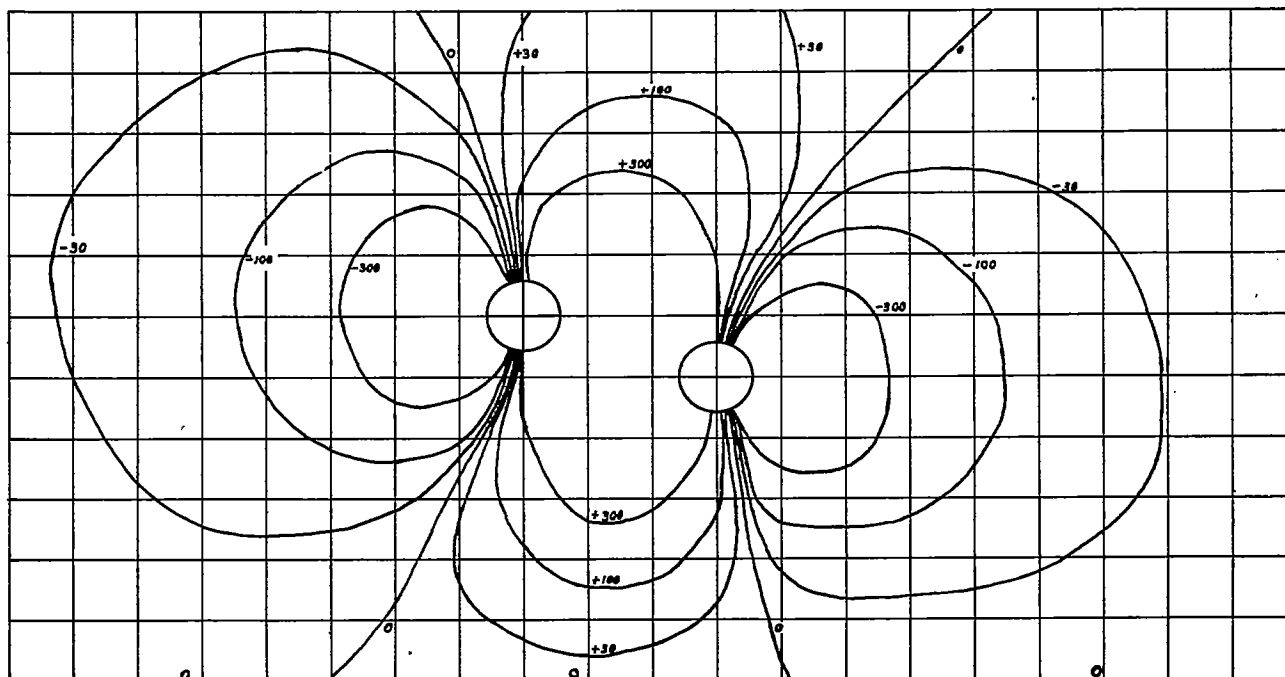


Figure 16b.- Two 33-coulomb charges of opposite sign at 5 and 6 kilometers above the surface, respectively.

DISTRIBUTION OF HORIZONTAL GRADIENTS